Cloning of chaperonin CCT γ subunit gene essential for retinotectal development by whole-genome subtraction

全ゲノムサブトラクション法による網膜視蓋分化因子シャペロニンCCTγ遺伝子のクローニング

Naoto Matsuda

松田　尚人

Contents

1 Abstract

Zebrafish *no tectal neuron (ntn)* mutant obtained by trimethylpsoralen (TMP) mutagenesis showed defects in tectal neuropil formation and small eyes. I carried out whole-genome subtraction between wild-type and mutant zebrafish genomes using the representational difference analysis (RDA) method. Nineteen subtraction products enabled me to construct genetic and physical maps of the *ntn* region. Direct selection of cDNAs using a YAC clone encompassing the *ntn* locus and RT-PCR analysis of transcripts identified a 143-bp deletion in the *cct3* gene encoding the γ subunit of chaperonin containing TCP-1 (CCT). Injection of antisense *cct3* morpholino oligonucleotides into zebrafish embryos induced characteristic *ntn* phenotypes including defects in retinal ganglion cell (RGC) differentiation and tectal neuropil formation. Moreover, injection of *cct3* mRNA successfully rescued *ntn* mutant embryos. These results suggest that RDA is an efficient and widely applicable cloning strategy in zebrafish genetics. The strong expression of the *cct3* mRNA started in the entire embryos by 12 hpf and was sustained thereafter, but there were no detectable abnormalities in body patterning and neurogenesis in *ntn* mutant embryos at 30 hpf. The expression patterns of transcription factor genes *ath5* and *brn3b* that are essential for the development and maintenance of RGCs were indistinguishable between wild-type and *ntn* mutant embryos, but those of early and late differentiation markers of RGCs, nicotinic acetylcholine receptor β3 and neurolin, were diminished in mutant embryos. Immunostaining of acetylated tubulin also revealed the impairment of RGC neurite extension. Thus, the *ntn* mutation of the *cct3* gene impaired the differentiation of retinal neuroepithelial cells to RGCs. Similarly, the expression of *brn3b* was normal in the tectum of *ntn* mutants, but tectal neuropil formation was abolished. These results suggest that the γ subunit of chaperonin CCT plays an essential role in retinotectal development.

2 Introduction

Forward genetics is a powerful approach for the understanding of development and function of the brain. Zebrafish (*Danio rerio*) is an excellent model organism for investigating gene function in vertebrates; external fertilization, transparent embryos and random mutagenesis techniques facilitate phenotype-driven forward genetic analyses (Eisen, 1996). Indeed, large-scale screening of zebrafish mutagenized by *N*-ethyl-*N*-nitrosourea (ENU) identified ~2400 mutations affecting development and behavior (Driever et al., 1996; Haffter et al., 1996). However, molecular cloning of ENU-induced mutant genes will require positional cloning and/or candidate gene approaches (Postlethwait and Talbot, 1997), since ENU induces predominantly substitution mutations (Mullins et al., 1994; Solnica-Krezel et al., 1994). Thus, availability of tightly-linked polymorphic markers will be rate-limiting to initiate chromosomal walking. In terms of cloning, insertion mutagenesis with pseudotyped retroviruses is a straightforward approach to obtain mutated genes (Gaiano et al., 1996). Hopkins and colleagues isolated more than 500 insertional mutants (Golling et al., 2002), but the efficiency of mutagenesis was still lower than ENU mutagenesis (Amsterdam et al., 1999).

Deletion mutagenesis is an alternative method to insertional mutagenesis, since deletions themselves will provide markers for the cloning of mutated genes by appropriate techniques such as whole-genome subtraction. Gamma- and X-rays are known to produce deletions in zebrafish. However, the size of deletions is so large as to involve several genes or they cause even chromosomal rearrangements (Chakrabarti, 1983; Mullins, 1994). 4,5',8-trimethylpsoralen (TMP) is a DNA cross-linking agent that can frequently induce small deletions in combination with UV irradiation in *Escherichia coli* and *Caenorhabditis elegans* (Sladek et al., 1989; Yandell et al., 1994; Liu et al., 1999). TMP mutagenesis has been proved to be efficient also in zebrafish (Ando and Mishina, 1998). In a pilot screen using TMP as a chemical mutagen, three mutant lines with abnormalities in the nervous system have been established. The *no tectal neuron (ntn)*^{jt5} mutation impairs the development of tectal neurons and eyes. The *edawakare*^{jt10} mutation affects the arborization of the trigeminal ganglion and Rohon-Beard sensory neurons. The *vibrato*^{jt12} mutation has defects in spontaneous contraction and touch response.

Representational difference analysis (RDA) is a powerful subtraction method which utilizes a subtractive hybridization method by using representations (amplicons) of the genomes that have a reduction in complexity (Lisitsyn and Wigler, 1993)(Fig. 1). Restriction fragments whose sizes and

sequences are suitable for PCR amplification are enriched in the amplicon, and other fragments remain unamplified. Deletion mutations should be particularly amenable to this analysis. In addition, restriction fragment length polymorphisms (RFLPs) can also be the basis for RDA products, when only one allele can be amplified. Two DNA samples are generated from pooled embryos based on their phenotypes from a segregating population from a single cross. Each pool contains individual embryos that are identical for a particular trait or genomic region but arbitrary at all unlinked regions. If RDA is performed with these pools, only differences in the vicinity of a locus of interest will be isolated.

In this thesis, I applied RDA to characterize the genomic region of the TMP-induced *ntn* mutation in an attempt to clone deleted fragments in the mutant genome or polymorphic markers between the wild-type and mutant genomes. Successful isolation of tightly linked polymorphic markers by the whole-genome subtraction method led to the construction of genetic and physical maps of the zebrafish genomic region responsible for retinotectal development. I identified a 143-bp deletion by RT-PCR in the *cct3* gene encoding the γ subunit of chaperonin containing TCP-1 (CCT, also called the TCP-1 ring complex or TriC). By phenotypic rescue and phenocopy experiments, I defined the *ntn* mutation of the *cct3* gene caused the mutant phenotype. These results revealed that chaperonin CCTγ controls specifically retinotectal development in zebrafish. The present results open a novel TMP mutagenesis-RDA cloning strategy of zebrafish forward genetics characterized by high efficiency and rapid cloning.

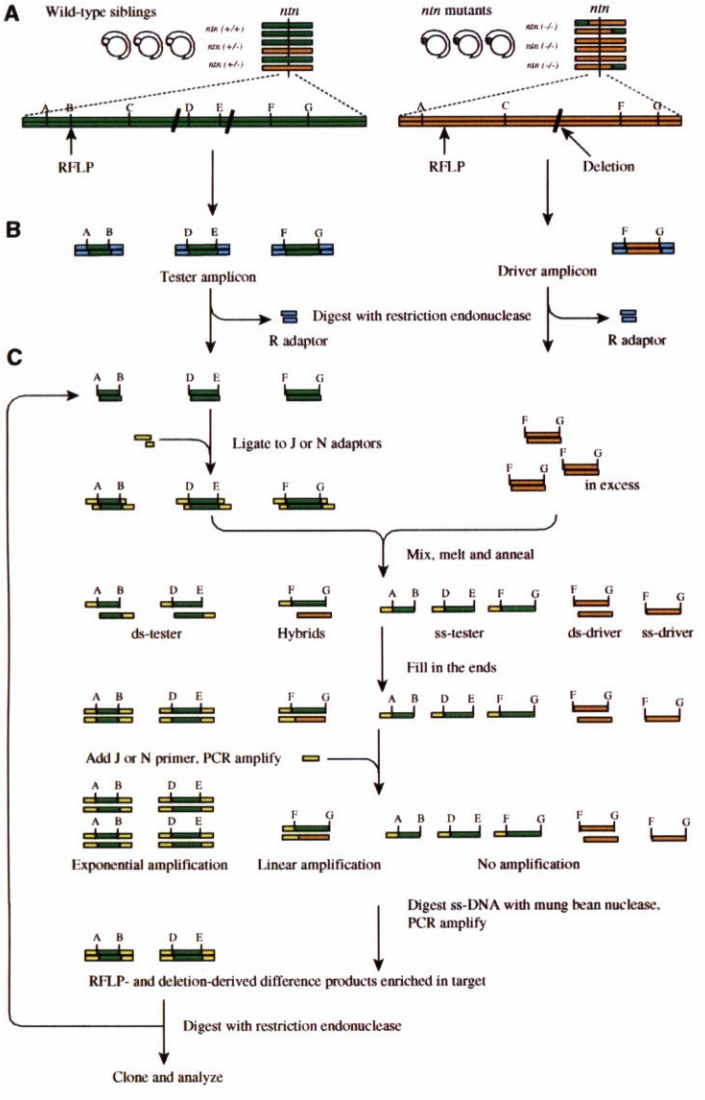

Figure 1. Schematic protocol for genetically directed representational difference analysis. **(A)** Pooled segregant analysis. By pooling embryos based on their phenotypes, only differences in genomic sequences liked to a locus of interest will be presented for subtraction. Green indicates genomic regions derived from wild-type embryos, orange *ntn* mutant embryos. A–G indicate cleavage sites of a given restiction endonuclease. Site B is lost in the mutant pool due to a polymorphism; sites D and E are absent in the mutant pool due to a deletion. **(B)** Representation: highly reproducible sampling of two genomic DNAs with a restriction endonuclease, ligation to R adaptors and whole-genome PCR of the short fragments only (fragments A–B, D–E and F–G). This step reduces complexity from genome to a subset (˜5–10% of the total genome). **(C)** Subtractive and kinetic enrichment with J or N adaptors. Modified from Lisitsyn and Wigler, 1993.

3 Methods

3.1 Strains and breeding of zebrafish

Zebrafish of the AB strain were raised and kept under standard conditions at ~26°C (Mullins et al., 1994). The *ntn* mutant line *jt5* was isolated by TMP mutagenesis previously (Ando and Mishina, 1998). The *ntn* mutant embryos at 3 days postfertilization (dpf) showed small eyes and turbid tectum. Mutation carriers were identified by random intercrosses and were then outcrossed to wild-type zebrafish of the AB strain. Mutant embryos were obtained by crossing heterozygous fish. The transgenic zebrafish line carrying the nicotinic acetylcholine receptor $\beta 3$ (nAChR$\beta 3$) gene promoter-driven enhanced green fluorescent protein (EGFP) expression vector (PAR-EGFP) was established previously (Tokuoka et al., 2002). Embryos were raised at 28.5°C in embryo rearing solution (ERS) (Easter and Nicola, 1996). For microscopic observation, 0.2 mM phenylthiocarbamide was added to ERS at 12 hours postfertilization (hpf) to prevent melanocyte pigmentation (Westerfield, 1995).

3.2 RDA procedure

Genomic DNAs were prepared from pools of 40 mutant embryos and 40 wild-type siblings and RDA was performed essentially as described (Lisitsyn et al., 1994; Lisitsyn and Wigler, 1995). Adaptor/primer sequences were designed according to the protocol (Lisitsyn and Wigler, 1995) with some modifications on their cohesive end sequences compatible for the restriction endonuclease (Table 1). One μg each of genomic DNAs was digested with *Bgl*II, *Eco*RI, *Hin*dIII, *Spe*I and *Xba*I, and were PCR-amplified with R primers to generate amplicons. The iterative hybridization-amplification step was repeated three times for *Bgl*II, *Eco*RI, *Spe*I or *Xba*I amplicons and four times for *Hin*dIII amplicons. J or N primers were used for odd and even hybridization-amplification steps, respectively. The annealing temperature of all 24-mer primers in PCR amplification is 72°C, except the J Bgl24 primer used in *Bgl*II and *Hin*dIII representations which has a 70°C annealing temerature. The resulting RDA products were digested with the corresponding restriction enzymes to remove adaptors, agarose gel-isolated and cloned into pBluescript II SK(+) (Stratagene). One μg each of amplicon and 5 μg each of genomic DNA digested with respective restriction enzymes were electrophoresed in 2% agarose gels and transferred to Hybond-N+ nylon membranes (Amersham). Membranes were hybridized with RDA products labeled using a random primed DNA

labeling kit (Roche) as probes.

3.3 Genetic mapping

Genomic DNA was extracted from 93 pools of five *ntn* mutant embryos obtained from crosses of heterozygous fish. One μg genomic DNA from each pool was digested with *Bgl*II, *Eco*RI, *Hin*dIII, *Spe*I or *Xba*I. Digested DNAs were PCR-amplified to generate amplicons as above. Southern blot hybridization analyses of amplicons with RDA products were performed. Genomic sequences flanking the RFLP sites of RDAjt5B430, RDAjt5B460 and RDAjt5E340 were cloned by vectorette-PCR using a GenomeWalker kit (Clontech), and primers were designed to identify cleaved amplified polymorphic sequences (CAPS); RDAjt5B430 RFLP site, 5′-TGGCGGTTC-ATTCTGCTGTGCGAC-3′ and 5′-CGACAAGACTTTTGTCAGGTAG-3′; RDAjt5B460 RFLP site, 5′-CAATACCGGCAACTTTCAAC-3′ and 5′-CAAGGACAAGAAATCATG-CC-3′; RDAjt5E340 RFLP site, 5′-GTCAAAATGCTCACTATACTAACTGCTGTC-3′ and 5′-AGTTTCGGCTTGGTTACGGAATCTC-3′.

Mapping of YD1 and YH2 loci was carried out by PCRs using primers flanking the deletions; YD1 locus, 5′-GACAGTGGAAATGCGGCTAT-3′ and 5′-TACCCATGTCTTCTGCGTAG-3′; YH2 locus, 5′-GGCCAGAGTTTACATAGG-GGT-3′ and 5′-GGTTTTTGCTGTGTCTGCCTG-3′.

Radiation hybrid (RH) mapping was performed on the Goodfellow zebrafish T51 RH panel (Research Genetics; Geisler et al., 1999) using the primers for the RDAjt5B460, RDAjt5E340 RFLP sites and YD1, YH2 loci.

3.4 Genomic DNA library screening and cDNA cloning

YAC clones D04128 and H0145 were obtained by PCR screening of a zebrafish YAC library (Resource Center/Primary Databank, Germany) with the primers for RDAjt5E340 RFLP site and their terminal sequences were determined as described (Zhong et al., 1998). PAC 10J03 and BAC 18M9 clones were isolated from zebrafish BAC and PAC libraries (Genome Systems) using ^{32}P-labeled RDAjt5B430 and RDAjt5E340 as probes, respectively. The inserts of these clones were sized by pulsed-field gel electrophoresis using CHEF-Mapper (BioRad). For YAC clonality analysis, the blot was probed with the ^{32}P-labeled YAC arm pRML plasmid. Zebrafish genomic DNA in YAC D04128 clone purified by pulsed-field gel electrophoresis was biotinylated using a random primed DNA labeling kit (Roche). A random primed zebrafish cDNA library was synthesized using RNA from zebrafish embryos at 36 hpf as templates (SuperScript Choice

Table 1: **Primers for RDA**

Enzyme	Name	Sequence
*Bgl*II	R Bgl24	5′-AGCACTCTCCAGCCTCTCACCGCA-3′
	R Bgl12	5′-GATCTGCGGTGA-3′
	J Bgl24	5′-ACCGACGTCGACTATCCATGAACA-3′
	J Bgl12	5′-GATCTGTTCATG-3′
	N Bgl24	5′-AGGCAACTGTGCTATCCGAGGGAA-3′
	N Bgl12	5′-GATCTTCCCTCG-3′
*Eco*RI	R Eco24	5′-AGCACTCTCCAGCCTCTCACCGAG-3′
	R Eco12	5′-AATTCTCGGTGA-3′
	J Eco24	5′-ACCGACGTCGACTATCCATGAACG-3′
	J Eco12	5′-AATTCTCGCATG-3′
	N Eco24	5′-AGGCAACTGTGCTATCCGAGGGAG-3′
	N Eco12	5′-AATTCTCCCTCG-3′
*Hin*dIII	R Hind24	5′-AGCACTCTCCAGCCTCTCACCGCA-3′
	R Hind12	5′-AGCTTGCGGTGA-3′
	J Hind24	5′-ACCGACGTCGACTATCCATGAACA-3′
	J Hind12	5′-AGCTTGTTCATG-3′
	N Hind24	5′-AGGCAGCTGTGGTATCGAGGGAGA-3′
	N Hind12	5′-AGCTTCTCCCTC-3′
*Spe*I	R Spe24	5′-AGCACTCTCCAGCCTCTCACCGCA-3′
	R Spe12	5′-CTAGTGCGGTGA-3′
	J Spe24	5′-ACCGACGTCGACTATCCATGAACA-3′
	J Spe12	5′-CTAGTGTTCATG-3′
	N Spe24	5′-AGGCAGCTGTGGTATCGAGGGAGA-3′
	N Spe12	5′-CTAGTCTCCCTC-3′
*Xba*I	R Xba24	5′-AGCACTCTCCAGCCTCTCACCGTT-3′
	R Xba12	5′-CTAGAACGGTGA-3′
	J Xba24	5′-ACCGACGTCGACTATCCATGAACT-3′
	J Xba12	5′-CTAGAACGCATG-3′
	N Xba24	5′-AGGCAGCTGTGGTATCGAGGGAGT-3′
	N Xba12	5′-CTAGAACCCTCG-3′

System, Invitrogen) and PCR-amplified after ligation to adapters 5′-TAGTCCGAATTCAAGCAAGAGCAGA-3′ and 5′-CTCTTGCTTGAATCGGACTA-3′. After preincubation with 2 μg sonicated zebrafish genomic DNA and 1 μg *Hae*III-digested yeast genomic DNA, 1 μg preamplified cDNA was hybridized with 100 ng biotinylated zebrafish genomic DNA in YAC D04128 clone as described (Del Mastro and Lovett, 1996). The sequences of the 5′ and 3′ regions of the *cct3* cDNA were obtained by 5′- and 3′-rapid amplification of cDNA ends (RACE) using a SMART cDNA kit (Clontech), respectively. The entire coding sequence of *cct3* cDNA was cloned into pCRII vector (Invitrogen) by RT-PCR with primers, 5′-TGTCCGGTACCGGTGATCTAAC-3′ and 5′-AAATGGATTTCTGATGAGAACGTTGT-3′ to yield pCRII-CCT3. The deletion mutation in the *cct3* mRNA was identified by sequencing RT-PCR products of mRNAs from ~200 *ntn* homozygous embryos and ~650 wild-type siblings at 50 hpf according to the protocol of the SuperScript Choice System (Invitrogen). The mutation in the *cct3* gene was confirmed by PCR on 100 ng genomic DNAs from ~300 wild-type siblings and ~100 *ntn* embryos with primers flanking the 143-bp deletion, 5′-GCCATGCAAGTGTGTCGTAATG-3′ and 5′-CTCAGAGAAGTGAGCACACGAATG-3′. Genotyping of embryos was performed using the same primer set.

3.5 In situ hybridization

The entire coding sequence of the zebrafish *brn3b/pou4f2* was obtained by RT-PCR using primers designed by searching its partial cDNA sequence and genomic sequence from the public databases, 5′-CGGTCGCAAATATGATGATG-3′ and 5′-ATGATTCCACATCCCCTTTG-3′, and was cloned into pCRII vector to yield pCRII-BRN3B (GenBank accession number AB122025). I carried out whole-mount in situ hybridization with antisense RNA probes prepared with a DIG RNA labeling kit (Roche), paraffin-embedding and sectioning of whole embryos as described previously (Mori et al., 1994; Jowett, 1999). Deparaffinized sections were counterstained with 0.5% methyl green for 10 min. Probes for *ath5/lakritz*, *dlx2*, *hlx1*, *krox20*, *myod*, *ntl*, *pax2.1/noi*, *shh* and *zash1* mRNAs were as described by Masai et al. (2000), Akimenko et al. (1994), Seo et al. (1999), Oxtoby and Jowett, (1993), Weinberg et al. (1996), Schulte-Merker et al. (1994), Krauss et al. (1991), Krauss et al. (1993) and Allende and Weinberg (1994), respectively.

3.6 Stainings

Whole-mount immunostaining of zebrafish embryos with anti-acetylated tubulin antibody (Sigma) were carried out as previously described (Hammerschmidt et al., 1996) except that Alexa 488 anti-mouse IgG antibody (Molecular Probes) was used as secondary antibody. Immunostaining of cryosectioned embryos using a monoclonal antibody zn5 (Oregon Monoclonal Bank), which recognizes a cell-surface protein neurolin, was performed as described (Masai et al., 2003). Terminal deoxynucleotide transferase-mediated dUTP nick-end labeling (TUNEL) was carried out in cryosections according to the manufacturer's protocol (ApopTag Apoptosis Detection Kit; Serologicals Corporation). Nuclei were counterstained with Sytox (Molecular Probes) diluted at 1:10000 with Tris-buffered saline. Dechorionated embryos were soaked in ERS containing 5 μg/ml acridine orange (Sigma) or 100 μM Bodipy-ceramide (Fl C5, Molecular Probes) and 2% DMSO for 30 min in the dark. The embryos were washed, anesthetized by 0.02% 3-aminobenzoic acid ethyl ester (tricaine, Sigma) and embedded in low-melting temperature agarose gels during microscopic observation. The eyes and tectum of Bodipy-ceramide-stained embryos were scanned by confocal microscopy.

3.7 Phenocopy and phenotypic rescue

The fluorescein-tagged morpholino oligonucleotide complementary to the nucleotide residues -16 to +9 of the zebrafish *cct3* mRNA (nucleotide residues are numbered from the putative translational initiation codon, GenBank accession number AF506209; Golling et al., 2002) was obtained from GeneTools. The antisense or control oligonucleotide at a concentration of 4 μg/μl in 1x Danieau buffer (Nasevicius and Ekker, 2000) was injected into the yolk of 1–4-cell stage wild-type or transgenic embryos carrying PAR-EGFP using a microinjector (IM-300, Narishige). Distribution of oligonucleotides in embryos was monitored under fluorescent microscopy. Fluorescence of EGFP was much stronger and easily distinguishable from that of fluorescein. Fluorescence of EGFP-labeled retinal ganglion cell (RGC) axons was observed as described (Tokuoka et al., 2002). The 1.8 kb *Eco*RV–*Spe*I fragment from pCRII-CCT3 was cloned into the *Stu*I and *Xba*I sites of pCS2+ vector (Turner and Weintraub, 1994) to yield pCS-CCT3. Capped *cct3* mRNA was prepared from 1 μg pCS-CCT3 linearized with NotI using an mMessage mMachine kit (Ambion). I injected 110–270 pg mRNA into the cytoplasm of embryos produced by crossing heterozygous fish.

4 Results

4.1 Representation difference analysis of the *ntn* mutation

Zebrafish *no tectal neuron* (*ntn*) mutants isolated by TMP mutagenesis showed degeneration of tectal neurons and eyes (Ando and Mishina, 1998). The ntn^{jt5} allele was of recessive inheritance and fully penetrant. If TMP mutagenesis induces deletions in the zebrafish genome as in *E. coli* and *C. elegans* (Sladek et al., 1989; Yandell et al., 1994; Liu et al., 1999), it would be possible to directly clone deleted DNA segments by subtraction between pooled wild-type and mutant genomes. I subtracted the mutant genome from the wild-type sibling genome by the RDA method (Lisitsyn and Wigler, 1993). Alternatively, RDA subtraction may allow us to obtain DNA segments tightly linked to the *ntn* locus if there were enough RFLPs inherent in the AB strain genome. Zebrafish genomic DNA was digested with various 6-bp recognizing restriction endonucleases and selected five enzymes which produced DNA fragments with short mean lengths appropriate for RDA. I prepared PCR-amplified DNA fragments (amplicons) of genomic DNA from pools of 40 *ntn* mutant embryos and 40 wild-type siblings using each of *Bgl*II, *Eco*RI, *Hin*dIII, *Spe*I and *Xba*I restriction enzymes. Whole-genome subtraction was carried out using amplicons from wild-type genome as the tester and those from *ntn* mutants as the driver. After three or four rounds of subtractive hybridization amplification, difference products became detectable as clearly visible bands in agarose gels from respective amplicons (Fig. 2A). The bands were cloned, and each clone was examined whether it was a true difference product by comparing its hybridizing signals to tester and driver amplicons (Fig. 2B). Of 24 products analyzed, 19 products hybridized to only tester amplicons, suggesting that they were true difference products. Two *Hin*dIII products hybridized to both tester and driver amplicons; three *Spe*I products showed smearing hybridization signals, because they contained repetitive sequences. Southern blot hybridization analysis of genomic DNA from *ntn* mutants and wild-type siblings showed that each RDA product hybridized with two fragments in the wild-type genome, but with only the larger one in the mutant genome digested by the corresponding restriction enzymes (Fig. 2C). Two hybridizing fragments were present also in the genome of the AB strain. These results suggest that all the RDA products resulted from RFLPs between the wild-type and *ntn* mutant genomes rather than deletions in the mutant genome. I thus obtained RFLP polymorphic markers linked to the *ntn* locus by genetically directed RDA. I summarized the results of analyses of the RDA products in Table 2.

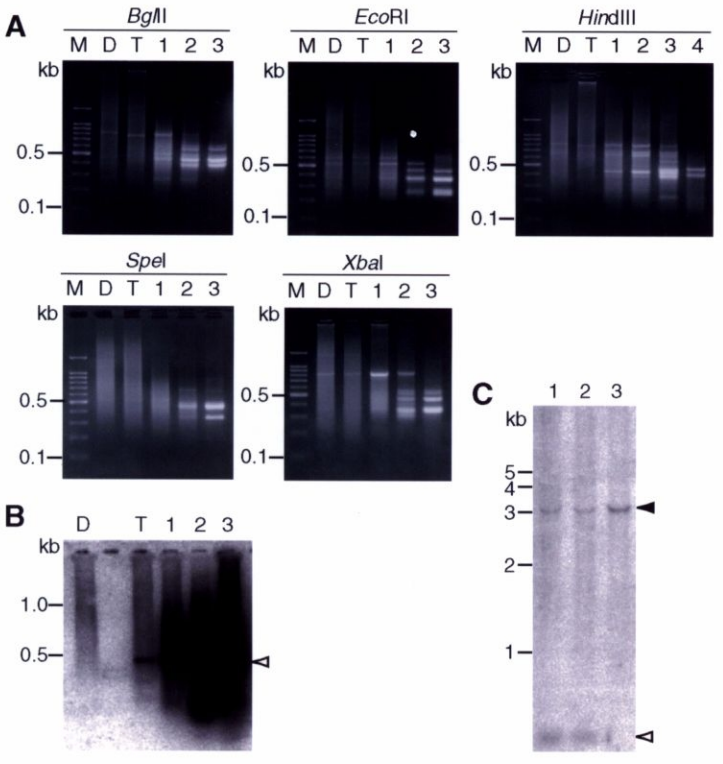

Figure 2. Whole-genome subtraction between *ntn* mutant embryos and wild-type siblings by RDA. **(A)** Analysis of RDA products by agarose gel electrophoresis. Driver and tester amplicons were prepared by digestion of genomic DNA from wild-type and *ntn* mutant embryos using *Bgl*II, *Eco*RI, *Hin*dIII, *Spe*I and *Xba*I restriction endonucleases, respectively. Lanes M, 100 bp DNA ladder as size markers; lanes D, driver amplicons; lanes T, tester amplicons; lanes 1–4, difference products of the first, second, third and fourth rounds of subtraction, respectively. **(B)** Southern blot hybridization of amplicons and RDA products using E420 as a probe. Lanes D, driver amplicon; T, tester amplicon; lanes 1–3, difference products of the first, second and third rounds of subtraction, respectively. An open arrowhead indicates the difference product E420 present in tester amplicon but absent in driver amplicon, which is gradually enriched in three rounds of subtraction. The sizes of markers in kb are indicated on the left. **(C)** Southern blot hybridization analysis of genomic DNA using RDA product E340 as a probe. Genomic DNAs from a wild-type fish of AB strain (lane 1), wild-type siblings (lane 2) and *ntn* mutant embryos (lane 3) were digested with *Eco*RI and hybridized to E340 probe. The sizes of markers in kb are indicated on the left. Filled and open arrowheads on the right indicate the 3.1-kb and 0.3-kb *Eco*RI-digested DNA fragments representing polymorphic alleles, respectively.

Table 2: **Summary of the RDA products**

Enzyme	Name (abbreviation)	Allele size (kb)		Type
		wild-type siblings	*ntn* homozygotes	
*Bgl*II	RDAjt5B430 (B430)	0.4, 3	0.4	RFLP
	RDAjt5B440 (B440)	0.4, 5	0.4	RFLP
	RDAjt5B460 (B460)	0.5, 6	0.5	RFLP
	RDAjt5B470 (B470)	0.5, 8	0.5	RFLP
	RDAjt5B610 (B610)	0.6, 8	0.6	RFLP
	RDAjt5B630 (B630)	0.7, 17	0.6	RFLP
*Eco*RI	RDAjt5E230 (E230)	0.3, 12	0.3	RFLP
	RDAjt5E340 (E340)	0.4, 3	0.4	RFLP
	RDAjt5E420 (E420)	0.4, 13	0.4	RFLP
	RDAjt5E550 (E550)	0.5, 9	0.5	RFLP
	RDAjt5E560 (E560)	0.6, 6	0.6	RFLP
*Hin*dIII	RDAjt5H400 (H400)	0.4, 8	0.4	RFLP
	RDAjt5H480 (H480)	0.5, 7	0.5	RFLP
	RDAjt5H510 (H510)	ND	ND	False
	RDAjt5H610 (H610)	ND	ND	False
*Spe*I	RDAjt5S270 (S270)	ND	ND	Repetitive sequence
	RDAjt5S390 (S390)	ND	ND	Repetitive sequence
	RDAjt5S450 (S450)	ND	ND	Repetitive sequence
	RDAjt5S610 (S610)	0.7, 1.1	0.7	RFLP
*Xba*I	RDAjt5X300 (X300)	0.3, 3.5	0.3	RFLP
	RDAjt5X350 (X350)	0.3, 2	0.3	RFLP
	RDAjt5X430 (X430)	0.4, 4	0.4	RFLP
	RDAjt5X520 (X520)	0.5, 2	0.5	RFLP
	RDAjt5X600 (X600)	0.6, 12	0.6	RFLP

4.2 Construction of genetic and physical maps

I then genetically selected polymorphic markers close to the *ntn* locus by Southern blot hybridization analysis of amplicons prepared from genomic DNA of 465 *ntn* mutant embryos. Genomic DNAs isolated from 93 pools of five mutant embryos were digested with the five restriction endonucleases used for RDA and amplicons were prepared. Blots of 93 amplicons were hybridized with the RDA products (Fig. 3A). The numbers of hybridizing signal-positive amplicons in the 93 amplicons were one for B460, H480, X300, X350 and X430, two for B440, B470, B610, B630, E230, E420, E560, S610 and X520, four for H400, six for X600, and eleven for E550. The genotyping of 93 mutant embryo pools revealed the positions of the polymorphic markers relative to the *ntn* locus (Fig. 3B). No recombinants among the *ntn*, B430 and E340 loci were found in 465 mutant embryos. The genetic mapping localized the *ntn* locus between the B440/E230/E560 and B460/H480/X300/X350/X430 loci.

I further determined the genotypes of 432 *ntn* mutant embryos for the B430 and E340 loci using CAPS markers (Fig. 3C). There was one recombination event between the *ntn* and B430 loci, the calculated genetic distance being 0.12 cM (95% confidence interval, 0.00–0.64 cM). On the other hand, I found no recombination events between the *ntn* and E340 loci. Thus, among isolated polymorphic RDA markers, E340 was the marker closest to the *ntn* locus.

I next screened zebrafish genomic libraries with E340 as a probe and obtained two YAC clones and one PAC clone (Fig. 4C). YAC H0145 contained a terminal sequence of BAC clone 18M9 obtained by screening with B430 as a probe. By comparing the 2.4-kb terminal sequences of YAC D04128 and the 2.9-kb terminal sequences of YAC H0145 with the corresponding genomic sequences of wild-type and *ntn* mutant embryos, we found 28-bp and 107-bp deletions in the *ntn* genome, designated as YD1 and YH2, respectively (Fig. 4C). Genotyping of 432 *ntn* mutant embryos by PCR using primers flanking the deletions in respective YAC ends identified one recombination event out of 864 meioses between the *ntn* and YH2 loci and one between the *ntn* and YD1 loci (Fig. 3C). I detected ten recombinations between the *ntn* and B460 loci by genotyping 432 *ntn* mutants using B460 CAPS marker. Thus, the relative order of markers around the *ntn* locus on the chromosome was B460–YH2–*ntn*/E340–YD1–B430 (Fig. 4A). These analyses localized the *ntn* locus within a 0.24 cM region between YH2 and YD1 markers.

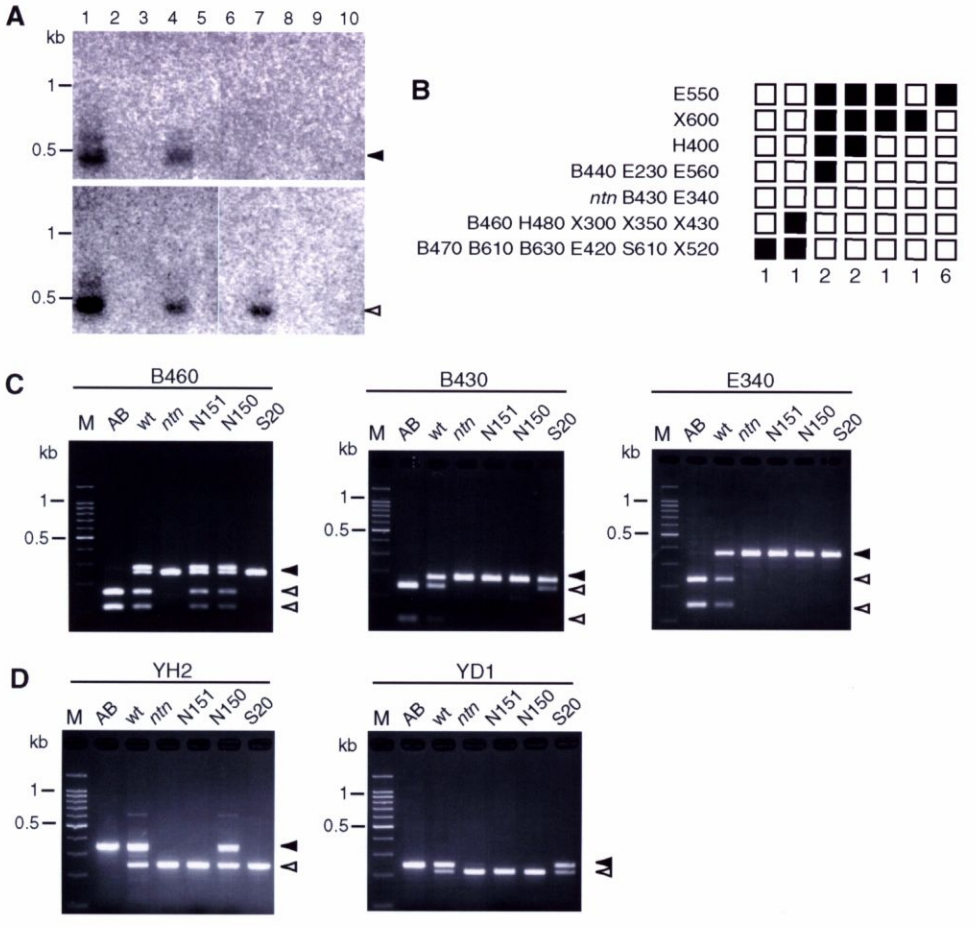

Figure 3. Genetic mapping of the RDA products linked to the *ntn* region. (A) An example of amplicon Southern blot hybridization analysis. Amplicons were prepared from *Bgl*II-digested genomic DNA from pools of five wild-type (lane 1) or *ntn* mutant (lanes 2-10) embryos. Blots were hybridized to B460 (upper) or B470 (lower) probe. Filled and open arrowheads indicate fragments in the amplicons hybridizing to B460 and B470 probes, respectively. **(B)** Amplicon Southern hybridization mapping of the *ntn* locus using polymorphic RDA products. Amplicons prepared from 93 pools of five *ntn* mutant embryos were hybridized to respective RDA products. Filled and open boxes indicate the presence and absence of amplicons hybridizing to RDA products, respectively. The numbers of pools containing recombinant(s) are given below. **(C)** Genetic mapping by CAPS. PCR products amplified from wild-type alleles are cleavable (open arrowheads), whereas those from mutant alleles are uncleavable (filled arrowheads). Lane AB, ~100 wild-type embryos of AB strain; lane wt, ~300 wild-type siblings; lane *ntn*, ~100 mutant embryos; lanes N151, N150 and S20, individual mutant embryos. Lane M shows 100 bp DNA ladder as size markers. **(D)** Genetic mapping using YH2 and YD1 deletion markers. Filled and open arrowheads represent wild-type and mutant alleles, respectively.

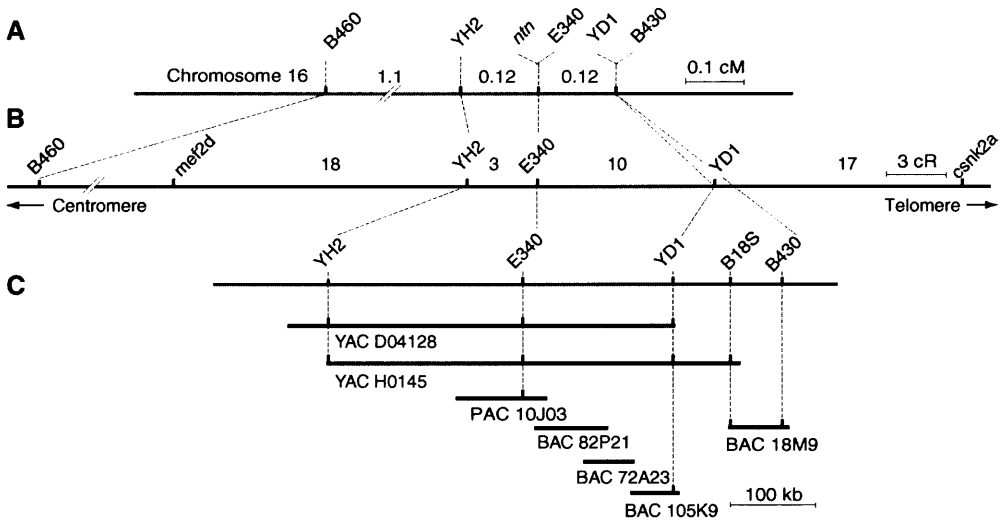

Figure 4. Construction of genetic, radiation hybrid and physical maps of the *ntn* region. Genetic, radiation hybrid and physical maps of the zebrafish *ntn* region on chromosome 16. **(A)** Genetic map of the *ntn* locus. Numbers in the genetic map indicate genetic distances in cM between the markers. **(B)** Radiation hybrid map of the *ntn* locus. csnk2a, the casein kinase 2a gene. mef2d, the myocyte enhancer factor 2D gene. Numbers in the radiation hybrid map indicate distances in cR between markers. **(C)** Physical map around the *ntn* locus is shown below with markers. Distances in the map are approximately to scale. Short horizontal lines below the physical map indicate YAC, PAC and BAC clones. BAC clones, 82P21, 72A23 and 105K9, were isolated by screening with C18orf1-like cDNAs as probes. B18S is a marker derived from the Sp6 end of BAC 18M9.

4.3 Transcripts from the *ntn* region

Using YAC D04128 as a probe, I isolated ~300 cDNA clones by screening a cDNA library prepared from zebrafish embryos at 36 hpf. Sequence analysis suggested that these clones encoded at least three genes. The first group of 26 cDNA clones and zebrafish ESTs (EST269466, fb13f04, fc26d03, fc72f03 and fe18d09) from the database of the Washington University zebrafish EST project encoded the subunit of zebrafish chaperonin CCT, which shared 87%, 86%, 85%, 70% and 58% amino acid sequence identities with the *Xenopus laevis*, mouse, human, *Drosophila melanogaster* and yeast counterparts, respectively (Chen et al, 1994; Kubota et al., 1994; Dunn and Mercola, 1996; Walkley et al., 1996a, b; Walkley and Malik, 1996). The second group of 5 cDNA clones encoded a putative protein having 69% amino acid sequence identity with human C18orf1, a transmembrane protein with a LDL receptor type A domain (Yoshikawa et al., 1998). A putative protein encoded by the third group of 7 cDNAs showed 32% amino acid sequence identity with mouse semaphorin 6C precursor (Kikuchi et al., 1999). One cDNA contained a single open reading frame, but there found no proteins homologous to the putative protein. The rest of the cDNA clones contained (CA)n dinucleotide repetitive sequences of various length and were not characterized further.

By RT-PCR analysis of mRNAs, I found a 143-bp deletion in the CCT subunit gene (*cct3*) transcript from the mutant embryos (Fig. 5A, B). The deletion was present in the *cct3* gene of mutant embryos, but not in the wild-type gene (Fig. 5C). The γ subunit of zebrafish CCT consisted of 543 amino acids and had five regions common to the CCT subunit proteins (Kim et al., 1994), the amino- and carboxyl-terminal equatorial ATPase domains, two intermediate domains and the apical substrate-binding domain (Fig. 5A). The *cct3* transcript in the mutant embryos completely lacked a putative ATPase motif and the reading frame was shifted by the deletion. There were no mutations within the coding sequences of three other candidate gene transcripts. I studied the expression of the *cct3* gene by in situ hybridization analysis (Fig. 5D). No transcripts were detectable in one-cell, shield and 90%-epiboly stage embryos at 0.2 hpf, 6 hpf and 9 hpf. At 12 hpf, strong hybridization signals for the *cct3* mRNA appeared in the entire embryos. The *cct3* mRNA was detected throughout the body at 24 hpf, and the brain, eyes and somites showed strong hybridization signals. At 36 hpf, hybridization signals for the *cct3* mRNA were observed in the entire brain and somites.

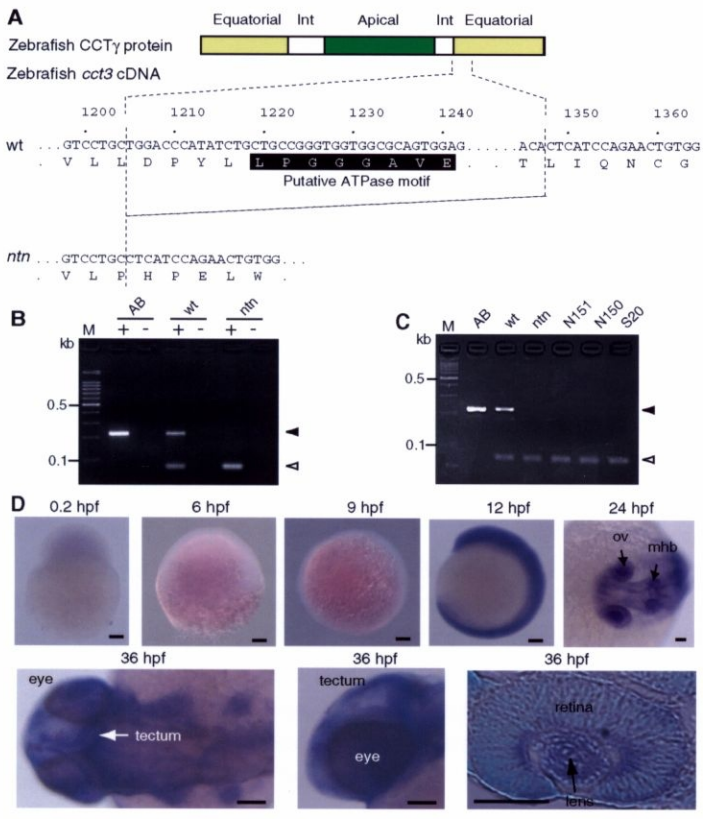

Figure 5. Identification of an internal deletion in the *ntn* mutant *cct3* gene and expression of the *cct3* mRNA in wild-type embryos during development. **(A)** A 143-bp internal deletion in the *cct3* transcript. The zebrafish CCT γ subunit is schematically shown above; the equatorial, apical and intermediate regions are indicated in boxes. The nucleotide sequences of a putative ATPase motif in the wild-type (wt) and mutant (*ntn*) *cct3* transcripts are shown below. The 143-bp deletion corresponding to the nucleotide residues 1205-1347 of the zebrafish *cct3* transcript is in the coding sequence for a putative ATPase motif of CCTγ. The deletion causes frame-shift and aberrant termination of translation. **(B)** RT-PCR analysis of the *cct3* gene transcripts from pools of ~1190 wild-type embryos of the AB strain (AB), ~650 wild-type siblings (wt) and ~200 mutant (*ntn*) embryos with (+) or without (-) a reverse transcriptase using primers flanking the 143-bp deletion. Lane M shows 100 bp DNA ladder as size markers. Filled and open arrowheads on the right indicate the 221-bp and 78-bp PCR products representing intact and deleted transcripts, respectively. **(C)** PCR analysis of genomic DNA from pools of ~100 wild-type embryos of AB strain (AB), ~300 wild-type siblings (wt), ~100 mutant (*ntn*) and three individual mutant (N151, N150 and S20) embryos using primers flanking the 143-bp deletion. Lane M shows 100 bp DNA ladder as size markers. Filled and open arrowheads on the right indicate the 221-bp and 78-bp PCR products representing the intact and deleted *cct3* genes, respectively. **(D)** Whole-mount in situ hybridization analysis of *cct3* mRNA at 0.2 hpf (one-cell stage), 6 hpf (shield stage), 9 hpf (90%-epiboly stage), 12 hpf, 24 hpf and 36 hpf. A section through the retina was shown for embryos at 36 hpf. mhb, midbrain-hindbrain boundary; ov, optic vesicle. Scale bars, 100 μm.

4.4 Identification of the *ntn* mutant gene

The characteristic phenotypes of *ntn* mutant embryos were selective impairment of development of the eyes and tectum at ~40 hpf (Ando and Mishina, 1998). At later stages (4 dpf), *ntn* mutants can be macroscopically distinguished from their wild-type siblings as having small eyes and turbidity in the developing tectum (Fig. 6A). There appeared no other abnormalities even at this stage except for small pectoral fins and some underdeveloped jaw skeletons in *ntn* mutant embryos. At 36 hpf, acridine orange staining (Abrams et al., 1993; Furutani-Seiki et al., 1996) showed strong signals selectively in the tectum of mutant embryos, suggesting apoptotic cell death (Fig. 6B). In fact, staining with Bodipy-ceramide, which was freely distributed in the interstitium between cells and delineated cellular membrane (Cooper et al., 1999), revealed patches of cell-free space probably reminiscent of engulfed dead cells in the tectum of mutant embryos at 46 hpf (Fig. 6C). Furthermore, the tectum of the mutant embryos at 48 hpf was hardly stained by antibody against acetylated tubulin (Fig. 6D), a marker protein of mature neurites (Chitnis and Kuwada, 1990), as described previously (Ando and Mishina, 1998). Neurites in the retinal ganglion cell layer were poorly developed and the bundle of the optic nerve was faint in *ntn* mutants (Fig. 6E). However, the staining patterns of other neurons such as axons of the anterior commissure neurons, hindbrain neurons, trigeminal ganglion cells and dorsal longitudinal fascicles were comparable between wild-type and mutant embryos (Fig. 6D, E).

To examine whether the mutation in the *cct3* gene was responsible for the *ntn* phenotypes, I injected an antisense morpholino oligonucleotide complementary to the *cct3* mRNA sequence encompassing the translation start codon into the wild-type embryos. The injected embryos showed small eyes at 4 dpf (Fig. 6F) and acridine orange staining in the tectum at 36 hpf (Fig. 6G). Bodipy-ceramide staining revealed loss of tectal cells (Fig. 6H). Anti-acetylated tubulin antibody immunostaining demonstrated that the formation of tectal neuropil and optic nerve was impaired in the embryos injected with an antisense morpholino oligonucleotide (Fig. 6I, J). Injection of a control morpholino oligonucleotide with the inverted antisense sequence exerted little effect on the development of the tectal and retinal neurons (Fig. 6F–J). These results suggest that suppression of CCT expression by the antisense morpholino oligonucleotide induces the characteristic phenotypes of *ntn* mutant embryos. I next injected wild-type *cct3* mRNA into one-cell stage embryos derived from crosses of heterozygous (+/-) fish to examine whether the *cct3* gene could rescue *ntn* mutant embryos. The injected embryos were stained with acridine orange for testing

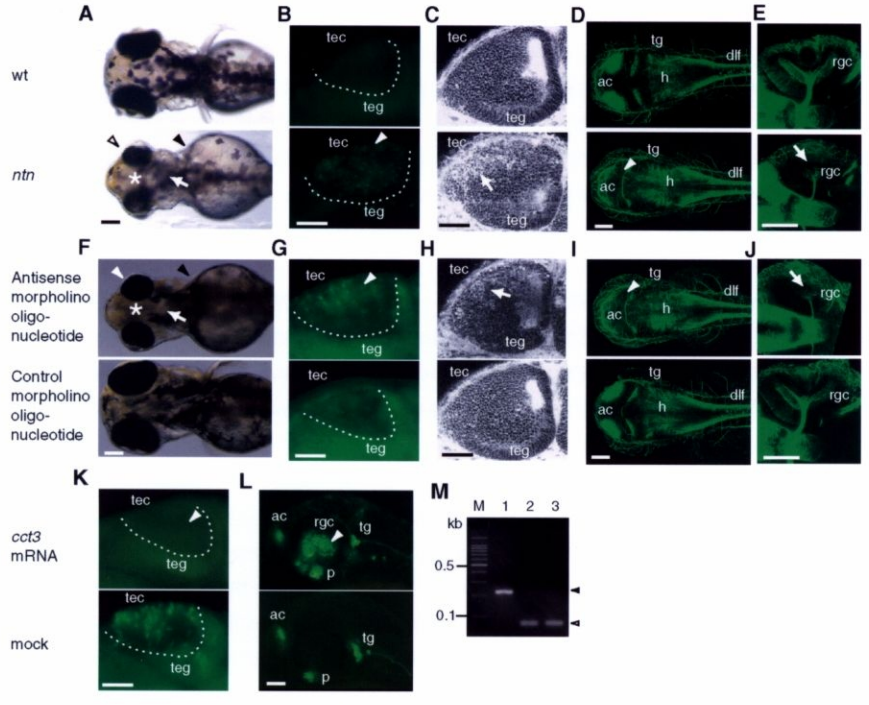

Figure 6. Phenocopy of the *ntn* mutation by a *cct3* antisense morpholino oligonucleotide and phenotypic rescue of *ntn* mutant embryos by the *cct3* mRNA injection. Dashed lines demarcate the tectum (tec). ac, anterior commissure neurons; dlf, dorsal longitudinal fasciculus; p, pituitary gland; rgc, retinal ganglion cells; teg, tegmentum; tg, trigeminal ganglion. **(A)** Dorsal view of wild-type (wt) and mutant (*ntn*) embryos at 4 dpf. An asterisk indicates the turbid tectum. Open and filled arrowheads indicate small eyes with protruding lens and poor pectoral fins in an *ntn* mutant embryo. An arrow indicates the reduced jaw. Scale bar, 50 μm. **(B)** Acridine orange staining of wild-type (wt) and mutant (*ntn*) embryos at 36 hpf. An arrowhead indicates significant staining signals in the tectum of an *ntn* mutant embryo. Scale bar, 50 μm. **(C)** Confocal optical section images of the tectum of Bodipy-ceramide-stained wild-type (wt) and mutant (*ntn*) embryos at 46 hpf. An arrow indicates patches of dead cells. Scale bar, 50 μm. **(D)** Confocal composite images of anti-acetylated tubulin immunostaining of wild-type (wt) and mutant (*ntn*) embryos at 48 hpf. An arrowhead indicates absence of staining signals in the tectum of an *ntn* mutant embryo. Scale bar, 50 μm. **(E)** Confocal composite images of the retinae of anti-acetylated tubulin immunostained wild-type (wt) and mutant (*ntn*) embryos at 48 hpf. An arrow indicates decreased numbers of RGCs and their axons in an *ntn* mutant embryo at 48 hpf. Scale bar, 50 μm.

(Figure 6 continued) **(F)** Dorsal view of *cct3* antisense and control morpholino oligonucleotide-injected embryos at 4 dpf. Open and filled arrowheads indicate small eyes with protruding lens and poor pectoral fins in an antisense oligonucleotide-injected embryo. An asterisk indicates the turbid tectum. An arrow indicates the reduced jaw. Scale bar, 50 μm. **(G)** Acridine orange staining of *cct3* antisense and control morpholino oligonucleotide-injected embryos at 36 hpf. An arrowhead indicates significant staining signals in the tectum of an antisense oligonucleotide-injected embryo. Scale bar, 50 μm. **(H)** Confocal optical section images of the tectum of Bodipy-ceramide-stained *cct3* antisense and control morpholino oligonucleotide-injected embryos at 48 hpf. An arrow indicates patches of dead cells. Scale bar, 50 μm. **(I)** Confocal composite images of anti-acetylated tubulin immunostaining of *cct3* antisense and control morpholino oligonucleotide-injected embryos at 48 hpf. An arrowhead indicates the absence of staining signals in the tectum of an antisense oligonucleotide-injected embryo. Scale bar, 50 μm. **(J)** Confocal composite images of the retinae of anti-acetylated tubulin immunostaining of *cct3* antisense and control morpholino oligonucleotide-injected embryos at 48 hpf. An arrow indicates decreased numbers of RGCs and their axons in an antisense morpholino-injected embryo at 48 hpf. Scale bar, 50 μm. **(K)** Acridine orange staining of *cct3* mRNA- and mock-injected *ntn* embryos at 36 hpf. An arrowhead indicates the absence of staining signals in the tectum of a *cct3* mRNA-injected *ntn* embryo. Scale bar, 50 μm. **(L)** Expression of nAChRβ3 gene promoter-driven EGFP in *cct3* mRNA- and mock-injected *ntn* embryos at 48 hpf. An arrowhead indicates the recovery of fluorescent signals in RGCs of a *cct3* mRNA-injected *ntn* embryo. Scale bar, 50 μm. **(M)** Genotyping of a wild-type sibling (lane 1), *cct3* mRNA- (lane 2) and mock-injected (lane 3) *ntn* embryos using primers flanking the 143-bp deletion in the *cct3* gene. Lane M shows 100 bp DNA ladder as size markers. Filled and open arrowheads on the right indicate the 221-bp and 78-bp PCR products representing the intact and deleted *cct3* genes, respectively.

the *ntn* mutant phenotypes (Fig. 6K). Among 77 embryos injected with *cct3* mRNA, only four embryos (5%) showed strong acridine orange staining in the tectum at 36 hpf and 73 embryos (95%) appeared normal, which deviated significantly from recessive inheritance (χ^2 test, $P < 0.001$). The genotyping of embryos with wild-type phenotypes revealed that 11 of 73 embryos were -/- at the *ntn* locus. The genotype at the *ntn* locus of 20 embryos was +/+ and that of remaining 42 embryos was +/-. Among 137 mock-injected embryos, 37 embryos (27%) showed the *ntn* mutant phenotypes (Fig. 6K) and 100 embryos (73%) exhibited the wild-type phenotypes, which was consistent with a recessive mode of inheritance (χ^2 test, $P = 0.70$). In 100 mock-injected embryos showing wild-type phenotypes, there were no embryos with -/- genotype at the *ntn* locus. All the embryos with wild-type phenotypes had genotypes of either +/+ or +/- at

the *ntn* locus. The development of the eyes at 3 dpf was normal in the embryos that did not show an increase in acridine orange staining in the tectum. These results suggest that injection of *cct3* mRNA rescued *ntn* mutant embryos. The nAChRβ3 gene is an early differentiation marker of RGCs (Matter-Sadzinski et al, 2001). To examine the differentiation of RGCs, I crossed the heterozygous *ntn* fish with a transgenic zebrafish carrying the nAChRβ3 gene promoter-directed EGFP expression vector (Tokuoka et al, 2002). Crossing of doubly transgenic fish with heterozygous *ntn* fish yielded homozygous mutant embryos with EGFP-labeled RGCs. Expression of EGFP signals in *ntn* embryos injected with *cct3* mRNA indicated the restoration of development of RGCs (Fig. 6L). In control mock-injected embryos, no EGFP signals appeared in the retina. Genotypes of *ntn* embryos injected with *cct3* mRNA showing wild-type phenotypes were confirmed to be -/- at the *ntn* locus by PCR using the primers flanking the deletion in the *cct3* gene (Fig. 6M).

4.5 Impairment of retinal development in *ntn* mutant zebrafish

Chaperones play an important role in folding of many proteins and CCT is a member of two major chaperone systems implicated in cytoplasmic protein folding in eukaryotes (Bukau and Horwich, 1998; Hartl and Hayer-Hartl, 2002). By 12 hpf, the strong expression of the *cct3* mRNA started in entire zebrafish embryos and continued thereafter (Fig. 5D). In the segmentation period (10–24 hpf), a variety of morphogenetic movements occur, the somites develop, the rudiments of the primary organs become visible and the overall body length of the embryo very rapidly increases (Kimmel et al., 1995). There might be subtle abnormalities in development of *ntn* mutants. Thus, I investigated whether there were any changes in body patterning or neurogenesis in *ntn* mutant embryos at 30 hpf by examining the expression patterns of several landmark genes. Two zebrafish homologs of the neurogenic gene *achaete-scute*, *zash1a* and *zash1b*, were strongly expressed in the entire neural retina (Fig. 7A) and in the midbrain and hindbrain (Fig. 7B) of both wild-type and *ntn* embryos at 30 hpf, respectively. Between wild-type and *ntn* embryos, there were no differences in the expression patterns of the homeobox genes *hlx1* in the midbrain (Fig. 7C), *dlx2* in the telencephalon and diencephalon (Fig. 7D), *krox20* in rhombomeres 3 and 5 (Fig. 7E), and *pax2.1* in the midbrain-hindbrain boundary (Fig. 7G). The expression patterns of *dlx2* in the pharyngeal arches (Fig. 7D), *shh* in midline structures (Fig. 7F), *pax2.1* in the optic stalk, otic vesi-

cle and pronephric duct (Fig. 7G), *ntl* in the notochord (Fig. 7H) and *myod* in the myotomes (Fig. 7I) were also comparable between wild-type and mutant embryos. Thus, the development of zebrafish embryos appeared to have proceeded normally until 30 hpf without the CCT γ subunit.

To examine the role of the *cct3* gene more precisely, we analyzed retinotectal development in *ntn* mutant embryos by Bodipy-ceremide and TUNEL staining and by expression patterns of differentiation markers. Zebrafish neural retina consists of proliferating neuroepithelial cells at 27 hpf (Hu and Easter, 1999). The differentiation of RGCs began in the ventronasal region of the retina at 28 hpf, then increasingly spread over the central region of the retina until 37 hpf (Hu and Easter, 1999; Malicki, 1999; Schmitt and Dowling, 1999; Tokuoka et al, 2002). Bodipy-ceremide staining showed that retinal neuroepithelial cells with elongated shapes were arranged radially and expanding in both wild-type and mutant embryos at 27 hpf and 36 hpf (Fig. 8A). No differences were detectable in cellular morphology and alignment between wild-type and mutant retinae at these stages. At 48 hpf, the number of retinal cells increased and their radial alignment became less prominent in wild-type embryos (Fig. 8A). However, the staining revealed a loss of significant numbers of cells in the inner region of the retina in mutant embryos, although differentiation of the lens vesicle to the lens and onionskin organization of the lens proceeded normally. Consistent with the results of Bodipy-ceremide staining, there were no significant differences in TUNEL staining between wild-type and *ntn* mutant embryos at 30 hpf and 36 hpf (Fig. 8B). At 48 hpf, clusters of TUNEL-positive cells were found in the peripheral region of the mutant retina, suggesting the occurrence of apoptotic cell death. On the other hand, the ciliary marginal zone where neuroepithelial cells proliferated was TUNEL-negative. These results suggest that the *ntn* mutation affected postmitotic developments rather than the proliferation of neuroepithelial cells. RGCs are the first postmitotic neurons to be born in the zebrafish retina (Hu and Easter, 1999). I thus examined retinal development by immunostaining with monoclonal antibody zn5, which recognizes a cell surface glycoprotein neurolin/DM-GRASP as an RGC differentiation marker (Trevarrow et al., 1990). The zn5 antibody staining showed strong signals in the central region of the wild-type retina at 48 hpf, whereas little staining was detectable in the *ntn* mutant retina, indicating the failure of RGC differentiation (Fig. 8C). Disturbance of retinal lamination was observed in mutant embryos at 72 hpf (data not shown). To further investigate the development of RGCs, we examined the expression of the nAChRβ3 gene, an early RGC differentiation marker (Matter-Sadzinski et al, 2001), by crossing *ntn* heterozygotes with transgenic zebrafish carrying the nAChRβ3

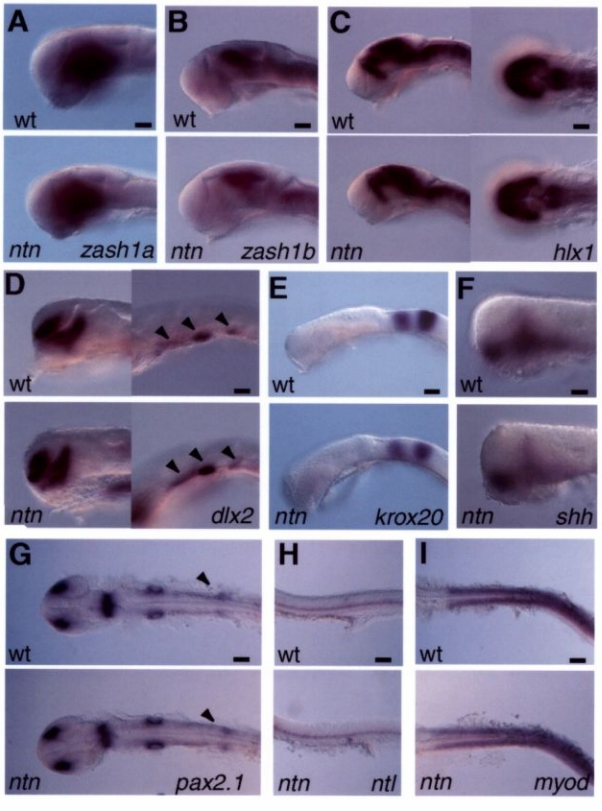

Figure 7. Expression patterns of developmental landmark genes in wild-type (wt, upper panels) and *ntn* mutant (lower panels) embryos at 30 hpf. (A) Lateral views of embryos stained by in situ hybridization with antisense *zash1a* probe. Scale bar, 100 μm. (B) Lateral views of embryos stained by in situ hybridization with antisense *zash1b* probe. Scale bar, 100 μm. (C) Lateral (left) and upper (right) views of embryos stained by in situ hybridization with antisense *hlx1* probe. Scale bar, 100 μm. (D) Lateral views of embryos stained by in situ hybridization with antisense *dlx2* probe. Arrowheads indicate pharyngeal arches. Scale bar, 100 μm. (E) Lateral views of embryos stained by in situ hybridization with antisense *krox20* probe. Scale bar, 50 μm. (F) Lateral views of embryos stained by in situ hybridization with antisense *shh* probe. Scale bar, 100 μm. (G) Lateral views of embryos stained by in situ hybridization with antisense *pax2.1* probe. Arrowheads indicate pronephric ducts. Scale bar, 50 μm. (H) Lateral views of embryos stained by in situ hybridization with antisense *ntl* probe. Scale bar, 50 μm. (I) Lateral views of embryos stained by in situ hybridization with antisense *myod* probe. Scale bar, 50 μm.

gene promoter-driven EGFP transgene (Tokuoka et al., 2002). In wild-type embryos, RGCs with EGFP signals appeared in the ventronasal region of the retina at 30 hpf, spread in the central region of the retina at 36 hpf and expanded in the inner retina to form the ganglion cell layer at 48 hpf (Fig. 8D). Retinal axons crossed the midline at 36 hpf and were extending towards the tectum at 48 hpf. In the mutant embryos, however, little EGFP signal was detectable in RGCs at 30 hpf, 36 hpf and 48 hpf (Fig. 8D). In contrast, EGFP signals in the trigeminal ganglion cells, Rohon-Beard sensory neurons and pituitary gland of mutant embryos were as strong as those of the wild-type embryos. The dorsal longitudinal fascicles and the axon fasciculation of trigeminal ganglion cells were comparable between wild-type and mutant embryos. Immunostaining with antibodies against acetylated tubulin, a general differentiation marker of neurons (Chitnis and Kuwada, 1990), showed that a small number of RGCs in the central region of the wild-type retina extended their axons at 30 hpf and 36 hpf (Fig. 8E). Anti-acetylated tubulin antibody stained RGC axons expanded in the inner retina and formed thick bundles at 48 hpf. On the other hand, little immunoreactivity to acetylated tubulin was detectable in the central region of the *ntn* mutant retina. At 36 hpf and 48 hpf, there were faint signals in the central region of the mutant retina, indicating poor development of RGCs.

I next examined the expression of the proneural basic helix-loop-helix transcription factor atonal homolog 5 (*ath5/lakritz)* as a marker for retinal neurogenesis by in situ hybridization. The expression pattern of *ath5* in the retina was comparable between wild-type and mutant embryos at 33 hpf (Fig. 9A). Brn3b/Pou4f2 acts downstream of Ath5 to promote retinal ganglion cell development (Liu et al., 2001), and is essential for the differentiation of RGCs (Xiang, 1998). I thus cloned a zebrafish homolog of *brn3b* from 36-hpf embryo cDNA. Deduced amino acid sequence of the zebrafish Brn3b protein showed 63% and 62% identities with those of human and mouse counterparts, respectively (Fig. 9B). I examined the expression of *brn3b* mRNA in the wild-type and mutant retinae at 36 hpf and 48 hpf (Fig. 9C). These results suggest that *ntn* mutation of the *cct3* gene exerted little effect on the commitment of retinal neuroepithelial cells to postmitotic retinal neurons but severely impaired the differentiation of retinal neuroepithelial cells to RGCs. Apoptosis of retinal cells observed after the impairment of RGC differentiation may be secondary effects of the *ntn* mutation.

Figure 8. Impairment of retinal development in *ntn* mutant embryos. **(A)** Confocal optical section images through the retina of Bodipy-ceramide stained wild-type (wt) and mutant (*ntn*) embryos at 27 hpf, 36 hpf and 48 hpf. An arrow indicates cell-free spaces. Scale bar 50 μm. **(B)** TUNEL staining of retinal sections of wild-type (wt) and mutant (*ntn*) embryos at 30 hpf, 36 hpf and 48 hpf. Scale bar, 50 μm. **(C)** Immunostaining with zn5 antibody (green) of retinal sections of wild-type (wt) and mutant (*ntn*) embryos at 30 hpf, 36 hpf and 48 hpf. Nuclei of retinal cells were counterstained with Sytox (red). Scale bar, 50 μm. **(D)** Confocal composite images of nAChR β3 gene promoter-driven EGFP signals in wild-type (wt) and mutant (*ntn*) embryos at 30 hpf, 36 hpf and 48 hpf in coronal view and those at 48 hpf in lateral view. Wild-type embryos have RGCs over the entire retina, whereas *ntn* mutants have sparse RGCs. Note that *ntn* mutants show EGFP signals in the trigeminal ganglion and Rohon-Beard sensory neurons and the pituitary gland. dlf, dorsal longitudinal fasciculus; on, optic nerve; p, pituitary gland; rb, Rohon-Beard neurons; tg, trigeminal ganglion. Scale bar, 100 μm. **(E)** Confocal composite images of immunostaining with anti-acetylated tubulin of retinal sections of wild-type (wt) and mutant (*ntn*) embryos at 30 hpf, 36 hpf and 48 hpf. Arrows indicate RGC axons. Scale bar, 50 μm.

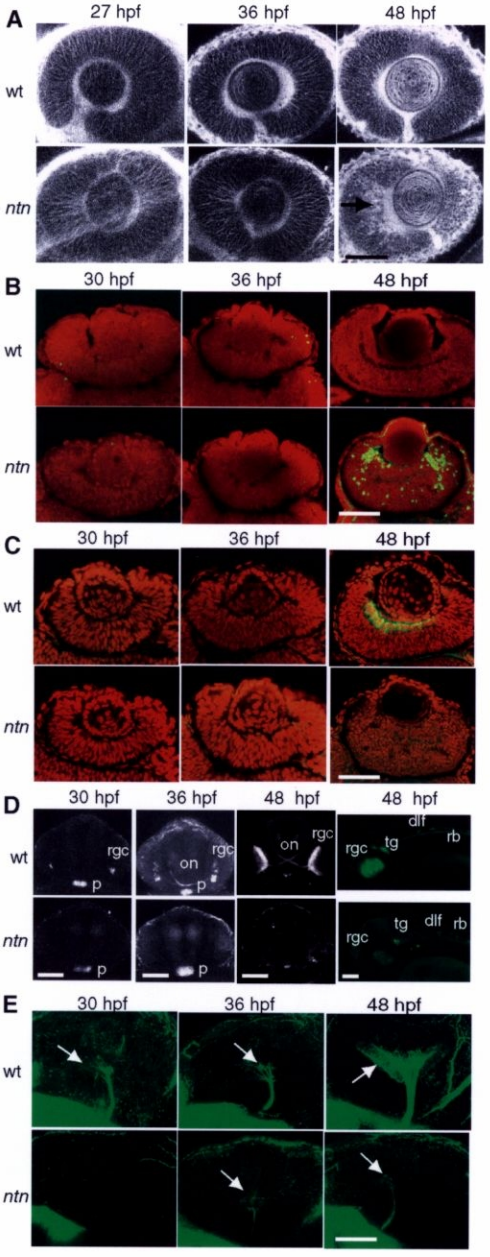

Figure 9. Expression of transcription factors essential for retinal development in *ntn* mutant embryos. **(A)** In situ hybridization of *ath5* mRNA in wild-type (wt) and mutant (*ntn*) embryos at 33 hpf. Ventral view. Scale bar, 100 μm. **(B)** Sequence alignment of the human, mouse and zebrafish Brn3b proteins. Black boxes indicate conserved amino acid identities; gray boxes indicate amino acid similarities. **(C)** In situ hybridization of *brn3b* mRNA in wild-type (wt) and mutant (*ntn*) embryos at 36 hpf and 48 hpf. Ventral view. Arrowheads indicate the RGC layer. Scale bar, 100 μm.

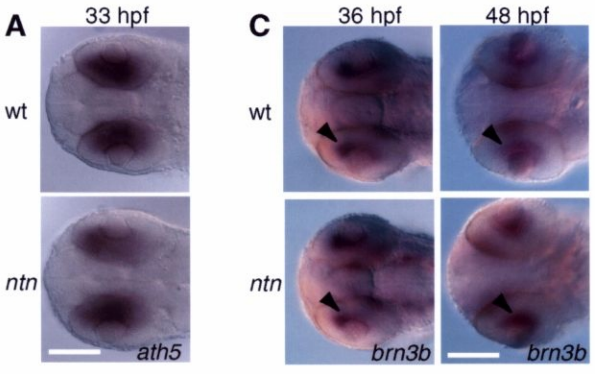

B

```
Human       MMMMSLNSKQAFSMPHGGSLHVEPKYSALHSTSPGSSAPIAPSASSPSSSSNAGGGGGGG
Mouse       MMMMSLNSKQAFSMPHAGSLHVEPKYSALHSASPGSSAPAAPSASSPSSSSNAGGGGGGG
Zebrafish   MMMMSLNSKQAFAMPHTS--LAEPKYSSLHSSSSSSTLTSNAPSSSCSSSR---------

Human       GGGGGGGGGRSSSSS-SSGSSGGGGSEAMRRACLPTPPSNIFGGLDESLLARAEALAAVD
Mouse       GGGGGGGRSSSSSSSGSGGSGGGGGSEAMRRACLPTPPSNIFGGLDESLLARAEALAAVD
Zebrafish   -------------HSSTISSSGGGSSEAMRRACLPTPPSNIFGGLDESLLARAEALAAVD

Human       IVSQSKSHHHHPPHHSPFKPDATYHTMNTIPCTSAASSSSVPISHPCALAGTHHHHHHHH
Mouse       IVSQSKSHHHHPPHHSPFKPDATYHTMNTIPCTSAASSSSVPISHPSALAGTHHHHHHHH
Zebrafish   IVSQTKSHHHPP-HHSPFKPDATYHTMNTLPCTSSSSSSSVPISHPSALAS---HHHHHH

Human       HHHHQPHQALEGELLEHLSPGLALG-AMAGPDGAVVSTPAHAPHMATMNPMHQAALSMAH
Mouse       HHHHQPHQALEGELLEHLSPGLALG-AMAGPDGTVVSTPAHAPHMATMNPMHQAALSMAH
Zebrafish   HHHHQPHQALEGDLLDHITPGLALAGAMAGPDGSVVSTPAHPAHMAGMNHMHQAAINMAH

Human       AHGLPSHMGCMSDVDADPRDLEAFAERFKQRRIKLGVTQADVGSALANLKIPGVGSLSQS
Mouse       AHGLPSHMGCMSDVDADPRDLEAFAERFKQRRIKLGVTQADVGSALANLKIPGVGSLSQS
Zebrafish   AHGLPSHMGCMSDVDADPRDLEAFAERFKQRRIKLGVTQADVGSALASLKIPGVGSLSQS

Human       TICRFESLTLSHNNMIALKPILQAWLEEAEKSHREKLTKPELFNGAEKKRKRTSIAAPEK
Mouse       TICRFESLTLSHNNMIALKPILQAWLEEAEKSHREKLTKPELFNGAEKKRKRTSIAAPEK
Zebrafish   TICRFESLTLSHNNMIALKPILQAWLEEAEKSHREKLNKPELFNGAEKKRKRTSIAAPEK

Human       RSLEAYFAIQPRPSSEKIAAIAEKLDLKKNVVRVWFCNQRQKQKRMKYSAGI
Mouse       RSLEAYFAIQPRPSSEKIAAIAEKLDLKKNVVRVWFCNQRQKQKRMKYSAGI
Zebrafish   RSLEAYFAIQPRPSSEKIAAIAEKLDLKKNVVRVWFCNQRQKQKRMKYSACV
```

4.6 Similar impairment of development of tectal cells

I also analyzed the development of tectal neurons by staining with Bodipy-ceremide (Fig. 10A). Zebrafish tectal cells proliferated over the whole extent of the tectal plate at 24 hpf and many tectal precursor cells turned into postmitotic cells forming the central differentiated zone by 48 hpf, while cells in the peripheral marginal zone still remained proliferative (Wullimann and Knipp, 2000). Large and round cells representing mitotically active cells (Cooper et al., 1999) were found along the edge of the tectum in wild-type embryos at 28 hpf and 36 hpf. During development from 28 hpf to 36 hpf, the total volume of the tectum remained relatively constant whereas each tectal neuron precursor became smaller in wild-type embryos. The ventricle between the tectum and the posterior tectal membrane became less prominent in wild-type embryos from 36 hpf to 40 hpf. There were no detectable abnormalities in the organization of the tectal neuroepithelium, alignment and mitotic cell images of tectal precursor neurons in *ntn* embryos at 28 hpf and 36 hpf. At 40 hpf, however, staining revealed cell-free spaces in the central zone of the tectum in mutant embryos. Consistently, TUNEL staining signals appeared in the tectum of mutant embryos at 40 hpf, but not at 30 hpf and 36 hpf (Fig. 10B). Immunostaining with anti-acetylated tubulin visualized the axons of trigeminal ganglion cells extending along the epidermis over the tectum and there were no significant differences in the immunostaining patterns of the tectum between wild-type and mutant embryos at 30 hpf and 36 hpf (Fig. 10C). At 40 hpf, immunostaining showed the formation of tectal neuropil by vigorous neurite extension of tectal neurons in wild-type embryos, but there was little staining in mutant embryos. On the other hand, the expression pattern of *brn3b* in tectal cells was comparable between wild-type and mutant embryos at 48 hpf (Fig. 10D), indicating the presence of tectal neurons. These results suggest that the *ntn* mutation of the *cct3* gene exerted little effect on the production of tectal cells but suppressed their differentiation to form tectal neuropil.

5 Discussion

5.1 TMP mutagenesis and RDA cloning

TMP mutagenesis procedures in zebrafish were developed in an attempt to facilitate the cloning of the mutated genes (Ando and Mishina, 1998). TMP in combination with UV irradiation forms interstrand cross-links

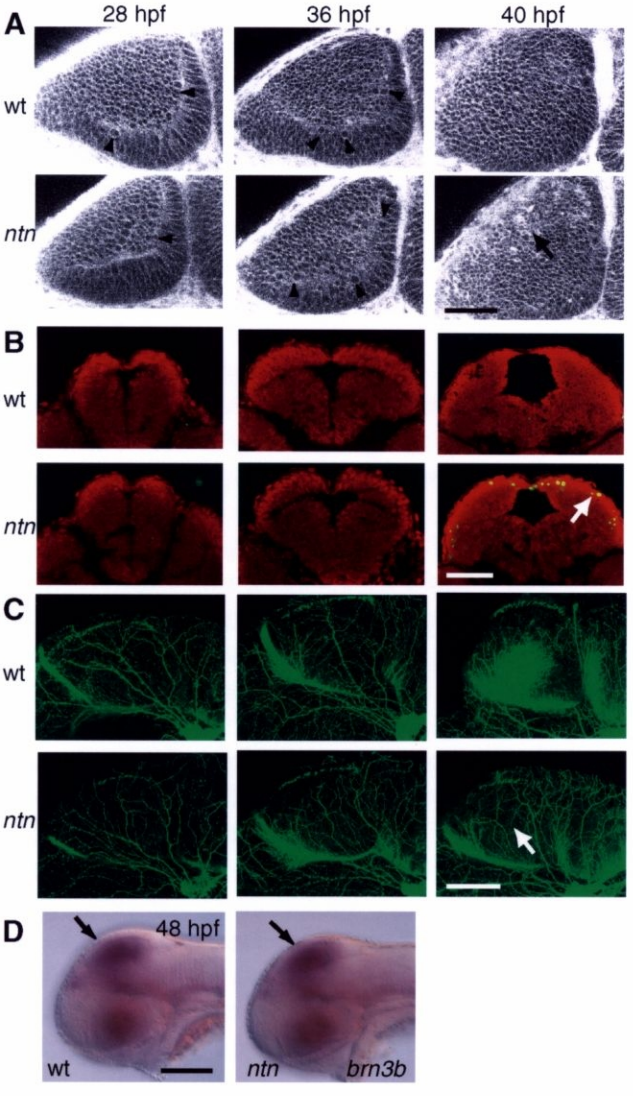

Figure 10. Impairment of tectal development in *ntn* mutant embryos. **(A)** Confocal optical section images of the tectum of Bodipy-ceramide stained wild-type (wt) and mutant (*ntn*) embryos at 28 hpf, 36 hpf and 40 hpf. An arrow indicates cell-free spaces. Arrowheads point large and round cells representing mitotically active cells. Scale bar 50 μm. **(B)** TUNEL staining of coronal sections through the tectum of wild-type (wt) and mutant (*ntn*) embryos at 30 hpf, 36 hpf and 40 hpf. An arrow indicates TUNEL-positive cells. Scale bar, 100 μm. **(C)** Confocal composite images of immunostaining with anti-acetylated tubulin antibody of wild-type (wt) and mutant (*ntn*) embryos at 30 hpf, 36 hpf and 40 hpf. An arrow indicates the absence of tectal neuropil. Scale bar, 50 μm. **(D)** In situ hybridization of *brn3b* mRNA in wild-type (wt) and mutant (*ntn*) embryos at 48 hpf. Dorsolateral view. Arrows indicate the tectum. Scale bar, 100 μm.

with DNA double helices and frequently results in deletions possibly via incomplete nucleotide excision and recombination repair in *E. coli* and *C. elegans* (Cimino et al., 1985; Sladek et al., 1989; Yandell et al., 1994). Subtraction of the mutant genome from the wild-type genome should yield deleted genes or tightly linked RFLP markers. The probability to directly clone the mutated gene by the whole-genome subtraction method of Lisitsyn and Wigler (1993) critically depends upon the size of a deletion and the presence of two restriction enzyme sites within the deleted segment. Because the sizes of deletions were 0.1 to 15 kb in *C. elegans* (Yandell et al., 1994; Jansen et al., 1997; Liu et al., 1999), I selected five restriction enzymes suitable for PCR-based amplicon preparations from zebrafish genomic DNA to increase the probability of success. Three to four rounds of subtraction between *ntn* and wild-type littermate genomes digested with respective restriction enzymes yielded one to six RDA products. I thus successfully isolated polymorphic markers tightly linked to the *ntn* locus, although none of the RDA products was deleted in the mutant genome. These markers enabled us to obtain YAC clones carrying the *ntn* locus and to identify a deletion in the chaperonin *cct3* gene as the cause of *ntn* mutation.

The present results demonstrate that the combination of TMP mutagenesis and genetically directed RDA provides a highly efficient and rapid cloning strategy for zebrafish forward genetics. Using RDA products from another TMP-induced *vibrato*^{ji12} mutant, a high-resolution physical map of a genomic region of 720 kb containing the mutant locus was successfully constructed (Sato and Mishina, 2003). The whole-genome subtraction method will be also applicable to zebrafish mutants induced by ENU. In addition to the 143-bp deletion in the *cct3* gene, there were two small deletions in ~5-kb *ntn* genomic region, indicating successful TMP deletion mutagenesis in zebrafish. Moreover, larger deletions were found in the genome of *edawakare*^{ji10} mutant zebrafish obtained by TMP mutagenesis (T. Morita, unpublished data). Thus, direct selection by RDA of the mutated genes from TMP-induced mutant fish would be feasible depending on the sizes of deletions induced. In *C. elegans*, deletion sizes were dependent on TMP concentration (Gengyo-Ando and Mitani, 2000).

5.2 Chaperonin CCTγ is essential for retinotectal development

In the present investigation, I identified the γ subunit of chaperonin CCT as an essential regulator of retinotectal development in zebrafish by whole-

genome subtraction cloning from TMP-induced *ntn* mutants. Induction of *ntn* phenotypes by injection of *cct3* antisense morpholino oligonucleotide into wild-type embryos and rescue of *ntn* mutants by injection of wild-type *cct3* mRNA clearly showed that the impaired retinotectal development in the *ntn* mutant fish was caused by the mutation in the chaperonin *cct3* gene. The *cct3* transcript in the mutant embryos completely lacked a putative ATPase motif and the reading frame was shifted by the deletion. Therefore, the translated mutant CCTγ protein appears to have a defective chaperone function. Available information suggests the presence of a single gene for the CCT γ subunit as well as the α, δ, ϵ, ζ, η and θ subunits in the zebrafish genome (`http://www.ensembl.org/Danio_rerio/`). A *cct3* zebrafish mutant was on the list of retroviral insertion mutants but no characterization was reported (Golling et al., 2002).

Molecular chaperones play an important role in folding of many proteins and CCT is a member of two major chaperone systems implied in cytoplasmic protein folding in eukaryotes (Bukau and Horwich, 1998; Hartl and Hayer-Hartl, 2002). In mammalian cells, ~15–20% of newly synthesized proteins transiently bind to Hsp70 and ~9–15% of them interact with CCT (Thulasiraman et al., 1999). Pharmacological inhibition of Hsp90, which cooperates with Hsp70 in folding of signal-transduction proteins (Young et al., 2001), was lethal and affected the development of various organs in zebrafish embryos (Lele et al., 1999). In addition, compromised Hsp90 activity in Drosophila and Arabidopsis caused a wide array of morphological variations, suggesting that Hsp90 acts as a capacitor for evolution (Rutherford and Landquist, 1998; Queitsh et al., 2002). Thus, it is surprising that the impairment of CCTγ caused defects specifically in coordinate retinotectal development of zebrafish. The causal relationship between CCTγ defect and the degeneration of retinal and tectal cells implies the importance of chaperones in neurodegenerative diseases (Slavotinek and Biesecker, 2001). CCT is a large cylindrical complex composed of eight different subunits providing physically defined compartments inside which a complete protein or a protein domain can fold while being sequestered from the cytosol (Kubota et al., 1995; Llorca et al., 1999). It is possible that the defect of the γ subunit in *ntn* mutants can be compensated by other CCT subunits to form functional CCT complex that assist folding of many proteins except for those specifically dependent on the γ subunit. The finding that the binding of actin to CCT is both subunit-specific and geometry-dependent (Vinh and Drubin, 1994; Llorca et al., 1999) may be consistent with this view. Major substrates of CCT are tubulin and actin in mammalian and yeast cells (Stoldt, et al., 1996; Thulasiraman et al., 1999). In fact, CCT is essential for mitosis and growth in budding yeast Saccha-

romyces cerevisiae and conditional mutations in individual CCT subunit genes affect biogenesis of tubulin and/or actin (Chen et al., 1994; Stoldt et al., 1996). However, there was no detectable expression of the *cct3* mRNA in zebrafish embryos from one-cell to 90%-epiboly stages when vigorous cell proliferation and gastrulation took place. The *cct3* mRNA was strongly expressed at 12 hpf in the entire embryo and sustained thereafter, but the defects in development of *ntn* mutant embryos became detectable only at ~30 hpf and specifically in the retinotectal system. Anti-acetylated tubulin immunostaining in most of neurons other than RGCs and tectal neuropil was comparable between wild-type and *ntn* mutant embryos. It is known that axonogenesis also involves actin biogenesis and polymerization (Chien et al., 1993). Thus, it is unlikely that the *ntn* mutation directly impaired the actin and/or tubulin biogenesis. Transducin α requires CCT activity for folding (Farr et al., 1993). However, unlike *ntn* mutants, zebrafish transducin α mutants showed morphologically normal retina (Brockerhoff et al., 2003).

5.3 *ntn* mutation impaired differentiation of retinal and tectal neurons

One may speculate that the effect of the *ntn* mutation of the CCTγ gene on the retinotectal development is rather nonspecific since CCT complex should assist folding of many proteins and since zebrafish mutants affecting both retina and tectum were frequently found in large-scale screens (Abdelilah et al., 1996; Furutani-Seiki et al., 1996). However, the specificity of the *ntn* phenotypes is three-fold. First, there were no detectable abnormalities in body patterning and neurogenesis in *ntn* mutant embryos at 30 hpf despite the fact that the strong expression of the *cct3* mRNA in the entire embryos started by 12 hpf and that very active developmental changes occurred in the segmentation period (10–24 hpf), including a variety of morphogentic movements, the development of somites and primary organ rudiments and rapid increase in overall body length of the embryo (Kimmel et al., 1995). Second, *ntn* phenotypes appeared specifically in the retina and tectum at ~2 dpf. At later stages (4 dpf), however, underdevelopment of pectoral fins and some jaw skeletons were noted in addition to small eyes and turbid tectum. Such abnormalities may be caused secondarily or may represent nonspecific effects. Third, a specific step in RGC differentiation is impaired in *ntn* mutants. The cellular organization of the retinal neuroepithelium at 27 and 36 hpf suggested that the formation of eye primordium, the proliferation of retinal cell progenitors

and retinal patterning proceeded normally in *ntn* mutant embryos. The expression patterns of transcription factors *ath5* and *brn3b* that are essential for the development and maintenance of RGCs (Erkman et al, 1996; Xiang, 1998; Brown et al., 2001; Kay et al., 2001; Matter-Sadzinski et al., 2001) were indistinguishable between wild-type and *ntn* mutant embryos, but those of early and late differentiation markers of RGCs, nAChRβ3 and zn5, were diminished in mutant embryos. Immunostaining of acetylated tubulin also revealed the impairment of RGC axon extension and optic nerve formation. Thus, *ntn* mutation of the *cct3* gene exerted little effect on the commitment of retinal neuroepithelial cells to postmitotic retinal neurons but severely impaired the differentiation of retinal neuroepithelial cells to RGCs. Similarly, the expression of *brn3b* was normal in the tectum of *ntn* mutants, but tectal neuropil formation was abolished. These results suggest that the γ subunit of chaperonin CCT plays an essential role in retinotectal development.

6 Acknowlegments

I am grateful to Professor M. Mishina for continuous mentoring, support and encouragement. I thank Dr. H. Mori and Dr. T. Yoshida for critical reading of the manuscript, Dr. T. Morita and Dr. T. Sato for helpful advice on RDA procedures, Dr. I. Masai and Dr. M. Take-uchi for advice on the analysis of retinal development, T. Kaneko and S. Fukuoka for technical assistance and K. Kinomoto for help in zebrafish breeding. I also thank Dr. A. Chitnis for *dlx2* cDNA, Dr. T. Jowett for *krox20* cDNA, Dr. S. Krauss for *shh* cDNA, Dr. I. Masai for *ath5* cDNA, Dr. S. Shulte-Merker for *ntl* cDNA, Dr. H. Takeda for *hlx1*, *myod* and *pax2.1* cDNAs, and Dr. E. Weinberg for *zash1a* and *zash1b* cDNAs.

7 References

Abdelilah, S., Mountcastle-Shah, E., Harvey, M., Solnica-Krezel, L., Schier, A. F., Stemple, D. L., Malicki, J., Neuhauss, S. C., Zwartkruis, F., Stainier, D. Y. et al. (1996). Mutations affecting neural survival in the zebrafish *Danio rerio*. Development 123, 217-27.

Abrams, J. M., White, K., Fessler, L. I. and Steller, H. (1993). Programmed cell death during *Drosophila* embryogenesis. Development 117, 29-43.

Akimenko, M. A., Ekker, M., Wegner, J., Lin, W. and Westerfield, M. (1994). Combinatorial expression of three zebrafish genes related to *distal-less*: part of a homeobox gene code for the head. J Neurosci 14, 3475-86.

Allende, M. L. and Weinberg, E. S. (1994). The expression pattern of two zebrafish *achaete-scute homolog (ash)* genes is altered in the embryonic brain of the *cyclops* mutant. Dev Biol 166, 509-530.

Amsterdam, A., Burgess, S., Golling, G., Chen, W., Sun, Z., Townsend, K., Farrington, S., Haldi, M. and Hopkins, N. (1999). A large-scale insertional mutagenesis screen in zebrafish. Genes Dev 13, 2713-2724.

Ando, H. and Mishina, M. (1998). Efficient mutagenesis of zebrafish by a DNA cross-linking agent. Neurosci Lett 244, 81-84.

Brockerhoff, S. E., Rieke, F., Matthews, H. R., Taylor, M. R., Kennedy, B., Ankoudinova, I., Niemi, G. A., Tucker, C. L., Xiao, M., Cilluffo, M. C. et al. (2003). Light stimulates a transducin-independent increase of cytoplasmic Ca2+ and suppression of current in cones from the zebrafish mutant *nof*. J Neurosci 23, 470-80.

Brown, N. L., Patel, S., Brzezinski, J. and Glaser, T. (2001). Math5 is required for retinal ganglion cell and optic nerve formation. Development 128, 2497-2508.

Bukau, B. and Horwich, A. L. (1998). The Hsp70 and Hsp60 chaperone machines. Cell 92, 351-366.

Chen, X., Sullivan, D. S. and Huffaker, T. C. (1994). Two yeast genes with similarity to TCP-1 are required for microtubule and actin function in vivo. Proc Natl Acad Sci USA 91, 9111-9115.

Chakrabarti, S., Streisinger, G., Singer, F. and Walker, C. (1983). Frequency of gamma-ray induced specific locus and recessive lethal mutations in mature germ cells of the zebrafish, *Brachydanio rerio*. Genetics 103, 109-124.

Chien, C. B., Rosenthal, D. E., Harris, W. A. and Holt, C. E. (1993). Navigational errors made by growth cones without filopodia in the embryonic *Xenopus* brain. Neuron 11, 237-251.

Chitnis, A. B. and Kuwada, J. Y. (1990). Axonogenesis in the brain of zebrafish embryos. J Neurosci 10, 1892-1905.

Cimino, G. D., Gamper, H. B., Isaacs, S. T. and Hearst, J. E. (1985). Psoralens as photoactive probes of nucleic acid structure and function: organic chemistry, photochemistry, and biochemistry. Annu Rev Biochem 54, 1151-1193.

Cooper, M. S., D'Amico, L. A., Henry, C. A. (1999). Confocal microscopic analysis of morphogenetic movements. Methods Cell Biol 59, 179-204.

Del Mastro, R. G. and Lovett, M. (1996). Isolation of coding sequences from genomic regions using direct selection. In Methods in Molecular Biology, vol. 68 (ed. J. Bolultwood), pp. 183-199. Totowa, NJ: Humana Press Inc.

Driever, W., Solnica-Krezel, L., Schier, A. F., Neuhauss, S. C., Malicki, J., Stemple, D. L., Stainier, D. Y., Zwartkruis, F., Abdelilah, S., Rangini, Z. et al. (1996). A genetic screen for mutations affecting embryogenesis in zebrafish. Development 123, 37-46.

Dunn, M. K. and Mercola, M. (1996). Cloning and expression of Xenopus CCTγ, a chaperonin subunit developmentally regulated in neural-derived and myogenic lineages. Dev Dyn 205, 387-394.

Easter, S. S., Jr. and Nicola, G. N. (1996). The development of vision in the zebrafish (*Danio rerio*). Dev Biol 180, 646-663.

Eisen, J. S. (1996). Zebrafish make a big splash. Cell 87, 969-977.

Erkman, L., McEvilly, R. J., Luo, L., Ryan, A. K., Hooshmand, F., O'Connell, S. M., Keithley, E. M., Rapaport, D. H., Ryan, A. F. and Rosenfeld, M. G. (1996). Role of transcription factors Brn-3.1 and Brn-3.2 in auditory and visual system development. Nature 381, 603-606.

Farr, G. W., Scharl, E. C., Schumacher, R. J., Sondek, S. and Horwich, A. L. (1997). Chaperonin-mediated folding in the eukaryotic cytosol proceeds through rounds of release of native and nonnative forms. Cell 89, 927-37.

Furutani-Seiki, M., Jiang, Y. J., Brand, M., Heisenberg, C. P., Houart, C., Beuchle, D., van Eeden, F. J., Granato, M., Haffter, P., Hammerschmidt, M. et al. (1996). Neural degeneration mutants in the zebrafish, *Danio rerio*. Development 123, 229-239.

Gaiano, N., Amsterdam, A., Kawakami, K., Allende, M., Becker, T. and Hopkins, N. (1996). Insertional mutagenesis and rapid cloning of essential genes in zebrafish. Nature 383, 829-832.

Geisler, R., Rauch, G. J., Baier, H., van Bebber, F., Brobeta, L., Dekens, M. P., Finger, K., Fricke, C., Gates, M. A., Geiger, H. et al. (1999). A radiation hybrid map of the zebrafish genome. Nat Genet 23, 86-89.

Gengyo-Ando, K. and Mitani, S. (2000). Characterization of mutations induced by ethyl methanesulfonate, UV, and trimethylpsoralen in the nematode *Caenorhabditis elegans*. Biochem Biophys Res Commun 269, 64-9.

Golling, G., Amsterdam, A., Sun, Z., Antonelli, M., Maldonado, E., Chen, W., Burgess, S., Haldi, M., Artzt, K., Farrington, S. et al. (2002). Insertional mutagenesis in zebrafish rapidly identifies genes essential for early vertebrate development. Nat Genet 31, 135-140.

Haffter, P., Granato, M., Brand, M., Mullins, M. C., Hammerschmidt, M., Kane, D. A., Odenthal, J., van Eeden, F. J., Jiang, Y. J., Heisenberg, C. P. et al. (1996). The identification of genes with unique and essential functions in the development of the zebrafish, Danio rerio. Development 123, 1-36.

Hammerschmidt, M., Pelegri, F., Mullins, M. C., Kane, D. A., van Eeden, F. J., Granato, M., Brand, M., Furutani-Seiki, M., Haffter, P., Heisenberg, C. P. et al. (1996). *dino* and *mercedes*, two genes regulating dorsal development in the zebrafish embryo. Development 123, 95-102.

Hartl, F. U. and Hayer-Hartl, M. (2002). Molecular chaperones in the cytosol: from nascent chain to folded protein. Science 295, 1852-1858.

Hu, M. and Easter, S. S. (1999). Retinal neurogenesis: the formation of the initial central patch of postmitotic cells. Dev Biol 207, 309-321.

Jansen, G., Hazendonk, E., Thijssen, K. L. and Plasterk, R. H. (1997). Reverse genetics by chemical mutagenesis in *Caenorhabditis elegans*. Nat Genet 17, 119-121.

Jowett, T. (1999). Analysis of protein and gene expression. Methods Cell Biol 59, 63-85.

Kay, J. N., Finger-Baier, K. C., Roeser, T., Staub, W. and Baier, H. (2001). Retinal ganglion cell genesis requires *lakritz*, a zebrafish *atonal* homolog. Neuron 30, 725-736.

Kikuchi, K., Chedotal, A., Hanafusa, H., Ujimasa, Y., de Castro, F., Goodman, C. S. and Kimura, T. (1999). Cloning and characterization of a novel class VI semaphorin, semaphorin Y. Mol. Cell. Neurosci. 13, 9-23.

Kim, S., Willison, K. R. and Horwich, A. L. (1994). Cytosolic chaperonin subunits have a conserved ATPase domain but diverged polypeptide-binding domains. Trends Biochem Sci 19, 543-548.

Kimmel, C. B., Ballard, W. W., Kimmel, S. R., Ullmann, B. and Schilling, T. F. (1995). Stages of embryonic development of the zebrafish. Dev Dyn 203, 253-310.

Krauss, S., Johansen, T., Korzh, V. and Fjose, A. (1991). Expression of the zebrafish paired box gene *pax[zf-b]* during early neurogenesis. Development 113, 1193-206.

Krauss, S., Concordet, J. P. and Ingham, P. W. (1993). A functionally conserved homolog of the *Drosophila* segment polarity gene *hh* is expressed in tissues with polarizing activity in zebrafish embryos. Cell 75, 1431-44.

Kubota, H., Hynes, G., Carne, A., Ashworth, A. and Willison, K. (1994). Identification of six Tcp-1-related genes encoding divergent subunits of the TCP-1-containing chaperonin. Curr Biol 4, 89-99.

Kubota, H., Hynes, G. and Willison, K. (1995). The chaperonin containing t-complex polypeptide 1 (TCP-1). Multisubunit machinery assisting in protein folding and assembly in the eukaryotic cytosol. Eur J Biochem 230, 3-16.

Lele, Z., Hartson, S. D., Martin, C. C., Whitesell, L., Matts, R. L. and Krone, P. H. (1999). Disruption of zebrafish somite development by pharmacologic inhibition of Hsp90. Dev Biol 210, 56-70.

Lisitsyn, N. and Wigler, M. (1993). Cloning the differences between two complex genomes. Science 259, 946-951.

Lisitsyn, N. and Wigler, M. (1995). Representational difference analysis in detection of genetic lesions in cancer. Methods in Enzymology 254, 291-304.

Lisitsyn, N. A., Segre, J. A., Kusumi, K., Lisitsyn, N. M., Nadeau, J. H., Frankel, W. N., Wigler, M. H. and Lander, E. S. (1994). Direct isolation of polymorphic markers linked to a trait by genetically directed representational difference analysis. Nat Genet 6, 57-63.

Liu, L. X., Spoerke, J. M., Mulligan, E. L., Chen, J., Reardon, B., Westlund, B., Sun, L., Abel, K., Armstrong, B., Hardiman, G. et al. (1999). High-throughput isolation of *Caenorhabditis elegans* deletion mutants. Genome Res 9, 859-867.

Liu, W., Mo, Z. and Xiang, M. (2001). The Ath5 proneural genes function upstream of Brn3 POU domain transcription factor genes to promote retinal ganglion cell development. Proc Natl Acad Sci USA 98, 1649-1654.

Llorca, O., McCormack, E. A., Hynes, G., Grantham, J., Cordell, J., Carrascosa, J. L., Willison, K. R., Fernandez, J. J. and Valpuesta, J. M. (1999). Eukaryotic type II chaperonin CCT interacts with actin through specific subunits. Nature 402, 693-6.

Macdonald, R., Barth, K. A., Xu, Q., Holder, N., Mikkola, I. and Wilson, S. W. (1995). Midline signalling is required for Pax gene regulation and patterning of the eyes. Development 121, 3267-3278.

Malicki, J. (1999). Development of the retina. Methods Cell Biol 59, 273-299.

Masai, I., Stemple, D. L., Okamoto, H. and Wilson, S. W. (2000). Midline signals regulate retinal neurogenesis in zebrafish. Neuron 27, 251-63.

Masai, I., Lele, Z., Yamaguchi, M., Komori, A., Nakata, A., Nishiwaki, Y., Wada, H., Tanaka, H., Nojima, Y., Hammerschmidt, M. et

al. (2003). N-cadherin mediates retinal lamination, maintenance of forebrain compartments and patterning of retinal neurites. Development 130, 2479-94.

Matter-Sadzinski, L., Matter, J. M., Ong, M. T., Hernandez, J. and Ballivet, M. (2001). Specification of neurotransmitter receptor identity in developing retina: the chick ATH5 promoter integrates the positive and negative effects of several bHLH proteins. Development 128, 217-231.

Mori, H., Miyazaki, Y., Morita, T., Nitta, H. and Mishina, M. (1994). Different spatio-temporal expressions of three *otx* homeoprotein transcripts during zebrafish embryogenesis. Mol Brain Res 27, 221-231.

Mullins, M. C., Hammerschmidt, M., Haffter, P. and Nusslein-Volhard, C. (1994). Large-scale mutagenesis in the zebrafish: in search of genes controlling development in a vertebrate. Curr Biol 4, 189-202.

Nasevicius, A. and Ekker, S. C. (2000). Effective targeted gene 'knockdown' in zebrafish. Nat Genet 26, 216-220.

Oxtoby, E. and Jowett, T. (1993). Cloning of the zebrafish *krox-20* gene (*krx-20*) and its expression during hindbrain development. Nucleic Acids Res 21, 1087-1095.

Postlethwait, J. H. and Talbot, W. S. (1997). Zebrafish genomics: from mutants to genes. Trends Genet 13, 183-190.

Queitsch, C., Sangster, T. A. and Lindquist, S. (2002). Hsp90 as a capacitor of phenotypic variation. Nature 417, 618-624.

Rutherford, S. L. and Lindquist, S. (1998). Hsp90 as a capacitor for morphological evolution. Nature 396, 336-342.

Sato, T. and Mishina, M. (2003). Representational difference analysis, high-resolution physical mapping and transcript identification of the zebrafish genomic region for a motor behavior. Genomics 82, 218-229.

Schmitt, E. A. and Dowling, J. E. (1999). Early retinal development in the zebrafish, *Danio rerio*: light and electron microscopic analyses. J Comp Neurol 404, 515-536.

Schulte-Merker, S., van Eeden, F. J., Halpern, M. E., Kimmel, C. B. and Nusslein-Volhard, C. (1994). *no tail (ntl)* is the zebrafish homologue of the mouse T (Brachyury) gene. Development 120, 1009-15.

Seo, H. C., Nilsen, F. and Fjose, A. (1999). Three structurally and functionally conserved Hlx genes in zebrafish. Biochim Biophys Acta 1489, 323-35.

Sladek, F. M., Melian, A. and Howard-Flanders, P. (1989). Incision by UvrABC excinuclease is a step in the path to mutagenesis by psoralen crosslinks in *Escherichia coli*. Proc Natl Acad Sci USA 86, 3982-3986.

Slavotinek, A. M. and Biesecker, L. G. (2001). Unfolding the role of chaperones and chaperonins in human disease. Trends Genet 17, 528-535.

Solnica-Krezel, L., Schier, A. F. and Driever, W. (1994). Efficient recovery of ENU-induced mutations from the zebrafish germline. Genetics 136, 1401-1420.

Stoldt, V., Rademacher, F., Kehren, V., Ernst, J. F., Pearce, D. A. and Sherman, F. (1996). Review: the Cct eukaryotic chaperonin subunits of *Saccharomyces cerevisiae* and other yeasts. Yeast 12, 523-529.

Thulasiraman, V., Yang, C. F. and Frydman, J. (1999). In vivo newly translated polypeptides are sequestered in a protected folding environment. EMBO J 18, 85-95.

Tokuoka, H., Yoshida, T., Matsuda, N. and Mishina, M. (2002). Regulation by glycogen synthase kinase-3β of the arborization field and maturation of retinotectal projection in zebrafish. J Neurosci 22, 10324-10332.

Trevarrow, B., Marks, D. L. and Kimmel, C. B. (1990). Organization of hindbrain segments in the zebrafish embryo. Neuron 4, 669-79.

Turner, D. L. and Weintraub, H. (1994). Expression of *achaete-scute homolog* 3 in *Xenopus* embryos converts ectodermal cells to a neural fate. Genes Dev 8, 1434-1447.

Vinh, D. B. and Drubin, D. G. (1994). A yeast TCP-1-like protein is required for actin function in vivo. Proc Natl Acad Sci USA 91, 9116-20.

Walkley, N. A., Demaine, A. G. and Malik, A. N. (1996). Cloning, structure and mRNA expression of human Cctγ, which encodes the chaperonin subunit CCTγ. Biochem J 313, 381-389.

Walkley, N. A. and Malik, A. N. (1996). Drosophila melanogaster P1 genomic clone DS05563 contains the chaperonin-encoding gene Cctγ. Gene 171, 221-223.

Walkley, N. A., Page, R. A. and Malik, A. N. (1996). Molecular characterisation of the Xenopus laevis chaperonin gene Cctγ. Biochim Biophys Acta 1309, 25-30.

Weinberg, E. S., Allende, M. L., Kelly, C. S., Abdelhamid, A., Murakami, T., Andermann, P., Doerre, O. G., Grunwald, D. J. and Riggleman, B. (1996). Developmental regulation of zebrafish MyoD in wild-type, *no tail* and *spadetail* embryos. Development 122, 271-80.

Westerfield, M. (1995). The Zebrafish Book. The University of Oregon Press.

Wullimann, M. F. and Knipp, S. (2000). Proliferation pattern changes in the zebrafish brain from embryonic through early postembryonic stages. Anat Embryol 202, 385-400.

Xiang, M. (1998). Requirement for Brn-3b in early differentiation of postmitotic retinal ganglion cell precursors. Dev Biol 197, 155-169.

Yandell, M. D., Edgar, L. G. and Wood, W. B. (1994). Trimethylpsoralen induces small deletion mutations in *Caenorhabditis elegans*. Proc Natl Acad Sci USA 91, 1381-1385.

Yoshikawa, T., Sanders, A. R., Esterling, L. E. and Detera-Wadleigh, S. D. (1998). Multiple transcriptional variants and RNA editing in C18orf1, a novel gene with LDLRA and transmembrane domains on 18p11.2. Genomics 47, 246-257.

Young, J. C., Moarefi, I. and Hartl, F. U. (2001). Hsp90: a specialized but essential protein-folding tool. J Cell Biol 154, 267-273.

Zhong, T. P., Kaphingst, K., Akella, U., Haldi, M., Lander, E. S. and Fishman, M. C. (1998). Zebrafish genomic library in yeast artificial chromosomes. Genomics 48, 136-138.